~~CONFIDENTIAL~~

RESEARCH MEMORANDUM

HIGH-SPEED WIND-TUNNEL TESTS OF A 1/78-SCALE MODEL OF THE LOCKHEED YP-80A AIRPLANE

By Robert N. Olson and
Leslie F. Lawrence

Ames Aeronautical Laboratory,
Moffett Field, Calif.

NATIONAL ADVISORY COMMITTEE
FOR AERONAUTICS

WASHINGTON
May 28, 1948

~~CONFIDENTIAL~~

Classification cancelled (or changed to Unclassified)

By authority of NASA Tech Pub Announcement
(OFFICER AUTHORIZED TO CHANGE)
74 30 Nov 54

By
NAME AND

GRADE OF OFFICER MAKING CHANGE)

10 Apr 61
DATE

NACA RM No. A7L24

[redacted]

NATIONAL ADVISORY COMMITTEE FOR AERONAUTICS

RESEARCH MEMORANDUM

HIGH-SPEED WIND-TUNNEL TESTS OF A 1/78-SCALE MODEL OF THE LOCKHEED YP-80A AIRPLANE

By Robert N. Olson and
Leslie F. Lawrence

SUMMARY

With the primary objective of determining the accuracy with which full-scale airplane characteristics can be predicted from high-speed wind-tunnel tests of airplane models of small scale, an investigation has been conducted to determine the high-speed performance and static longitudinal stability and control characteristics of a 1/78-scale model of the Lockheed YP-80A airplane.

High-speed aerodynamic characteristics are presented for speeds up to a Mach number of 0.96. Comparisons are made of the relative aerodynamic characteristics of the 1/78-scale model, a 1/3-scale model, and a full-scale YP-80A airplane. These comparisons reveal prematurely occurring lift and drag force breaks for the 1/78-scale model, with the lift loss and drag rise following the force breaks less severe than indicated by 1/3-scale and flight data. Tests made to visualize the flow within the boundary layer of the 1/78-scale model revealed a very long laminar boundary-layer run over the wing consistent with the scale of the tests. It is concluded that the Reynolds number effect on 1/78-scale results at high subsonic speeds is such as to permit its use solely as a qualitative measure of the full-scale aerodynamic characteristics of an airplane.

Results of the stability investigation revealed a region of static longitudinal instability to be present for the 1/78-scale YP-80A model at moderately high lift coefficients in the Mach number range of 0.81 to 0.90. An abrupt pitch-up motion, evident for moderate lift coefficients in this Mach number range (0.8 to 0.9) appeared in the 1/3-scale and full-scale tests only at the limiting Mach number of the tests (approximately 0.85 Mach number). This region of instability was effectively eliminated for the 1/78-scale model by sweeping back the leading edges of the horizontal

[redacted]

[redacted]

and vertical tail surfaces 45°. Beyond a Mach number of 0.9, a severe diving tendency accompanied by a rapid increase in longitudinal stability was apparent for both the conventional and swept-back-tail configurations.

Longitudinal-control tests of the conventional 1/78-scale YP-80A configuration indicated ineffectiveness of the elevators for a 4° deflection, presumably a result of the low scale of the tests. For an 8° elevator deflection the effectiveness was adequate over the speed range investigated except for lift coefficients near 0.4 where the effectiveness dropped off rapidly beyond a Mach number of 0.81.

Although, quantitatively, prediction of full-scale flight characteristics from the present small-scale results is difficult, trends in lift and drag forces and longitudinal stability and control characteristics are indicated which should be of considerable value to groups contemplating the test flying of conventional aircraft in the range of Mach numbers corresponding to those of the present tests.

INTRODUCTION

Investigations of Reynolds number effects on the aerodynamic characteristics of airfoil sections have indicated the unreliability of using low-scale data to predict full-scale characteristics at subcritical speeds (e.g., reference 1). However, Ferri, from the airfoil tests of reference 2 wherein the Reynolds number range from 150,000 to 500,000 was investigated, concluded that the significance of Reynolds number decreased beyond the critical Mach number, becoming virtually unimportant for Mach numbers near unity. A comparison of the low-scale Italian results with the lift and drag characteristics obtained at high scale (Reynolds number 6,000,000) showed large discrepancies, but Ferri attributed this lack of agreement to the differences in the testing techniques and equipment. Some support was given to Ferri's contention when it was found (reference 3) that the maximum lift of airfoils above about 0.5 Mach number was quite independent of scale.

To assess more thoroughly the effect of scale on the accuracy of prediction of full-scale characteristics from small-scale model tests, the present investigation of a small-scale airplane model was undertaken in the Ames 1- by 3½-foot high-speed wind tunnel. The Lockheed YP-80A airplane was chosen as the typical high-speed airplane to be used for this investigation because of the need for data on the high-speed performance characteristics of this airplane at speeds in the supercritical speed region beyond 0.85 Mach number

(the limit of previous wind-tunnel tests), and because of the availability of comparative data from both 1/3-scale model tests (reference 4) and full-scale flight tests (reference 5 and unpublished data on file at the Ames Laboratory).

The investigation was conducted over a Mach number range of 0.50 to 0.96 with a corresponding Reynolds number variation of 270,000 to 370,000. Tests were included to determine the static longitudinal stability and control characteristics of the 1/78-scale model to be analyzed prior to intended flight testing of the YP-80A airplane to higher transonic speeds than previously attained. Also included were tests to evaluate the effects on the longitudinal stability characteristics of sweeping back the horizontal and vertical-tail surfaces. These tests are of interest as regards stability characteristics in that speeds are attained well in excess of the critical Mach number of both the wing and the tail surfaces; whereas in most previous investigations the test Mach numbers have been well beyond the critical Mach number of the wing only.

Thus it was hoped to determine the extent to which high-speed wind-tunnel tests made at low scales could be used to predict full-scale flight characteristics, and to give an insight into the stability and control problems to be encountered at flight speeds in the supercritical region beyond the limits of previous investigations.

SYMBOLS

The following symbols are used in this report:

V	free-stream velocity, feet per second
ρ	free-stream mass density, slugs per cubic foot
q	free-stream dynamic pressure $(\frac{1}{2}\rho V^2)$, pounds per square foot
M	Mach number
R	Reynolds number
S	wing area, square feet
M.A.C.	mean aerodynamic chord, feet
C_D	drag coefficient $\left(\frac{\text{drag}}{qS}\right)$

[redacted]

C_L lift coefficient $\left(\frac{\text{lift}}{qS}\right)$

C_N normal-force coefficient $\left(\frac{\text{normal force}}{qS}\right)$

C_m pitching-moment coefficient $\left(\frac{\text{pitching moment}}{qS\ \text{M.A.C.}}\right)$

ΔC_m increase in pitching-moment coefficient

α angle of attack of the fuselage reference line, degrees

α_o angle of attack of the fuselage reference line for zero lift, degrees

δ_e elevator angle with respect to the stabilizer chord, degrees

p local static pressure, pounds per square foot

p_o free-stream static pressure, pounds per square foot

P pressure coefficient $[(p-p_o)/q]$

APPARATUS AND TESTS

A 1/78-scale model of the Lockheed YP-80A airplane, shown completely assembled in figure 1, was made in three sections as indicated in the exploded view of figure 2. The split construction of the fuselage was necessary to permit the installation of a strain gage for measuring pitching moments of the model. A schematic drawing of this installation is presented in figure 3. The tail unit was made detachable to permit testing of different tail assemblies without constructing a complete model for each configuration. A separate brass tail unit was constructed for each of five separate configurations: one of the conventional configurations with each of 0°, −4°, and −8° elevator deflections, a fourth unit having 45° leading-edge sweepback of both the horizontal- and vertical-tail surfaces, and a fifth comprising the tail-off condition. These tail assemblies are shown in figure 4. The wing and fuselage sections of the model were machined from steel and the entire model was cadmium plated and polished. After assembly all screw holes were filled with a glazing putty and smoothed.

The model was supported by tapered steel stings having a 3/32-inch diameter hole drilled through the center to permit passage of the electric leads for the pitching-moment strain

gage situated within the model. Angle-of-attack variation was accomplished by mounting the model successively on each of five bent stings.

The sting was mounted on a strain-gage balance beam supported by four cantilever springs riding on bearing ways fastened to the balance housing. This housing completely shrouded the beam and was held in position at the center line of the tunnel by means of steel cables fixed to the tunnel walls. The relative sizes and positions of the model, support, and balance are indicated in figure 5.

In figure 6 is presented a three-view sketch of the model, the principal dimensions of which are given in the appendix.

Force readings were taken through a Mach number range from 0.500 through 0.960, the Mach number at which a normal shock wave formed at the balance boom choking the air flow. Lift, drag, and pitching-moment measurements were made for the conventional configurations for nominal angles of attack of -2°, 0°, 2°, 4°, and 6° for elevator deflections of 0°, -4°, and -8°. The tail-off and swept-back-tail configurations were tested through the same angle-of-attack and Mach number ranges.

The average Reynolds numbers based on the mean aerodynamic chord of the wing for this test are given in figure 7 as a function of Mach number.

Tests were made with a 10-percent-chord strip of carborundum grains glued to the upper surface of the wing successively at the 50- and the 20-percent-chord stations of the model in an effort to fix the transition from laminar to turbulent flow. In a further effort to increase the effective Reynolds number, a grid of bars was installed just upstream of the test section to increase the turbulence of the air stream. A liquid-film method for measuring transition, essentially a visual method for determining the nature of the flow within the boundary layer, was employed in conjunction with this investigation. This method, described in detail in reference 6, is based on the fact that the greater the surface shear, the greater the rate of evaporation of a liquid film on the surface of the model. Runs were made through the Mach number range for 0° and 4° angles of attack with and without the turbulence grid installed and with carborundum glued to the upper surface of the left wing at the 20-percent-chord station.

The tests were conducted in the Ames 1- by $3\frac{1}{2}$-foot high-speed wind tunnel, a low-turbulence, two-dimensional-flow, single-return-passage wind tunnel powered by two 1000 horsepower electric motors.

REDUCTION OF DATA

All forces and moments were measured with respect to the wind axis and are presented in the form of lift, drag, and pitching-moment coefficients. To obtain these results, balance readings were multiplied by previously determined calibration constants to give the forces parallel and perpendicular to the wind axis and the pitching moment about a point at 25 percent M.A.C. on the fuselage reference line. The strain-gage balance calibrations were repeated at frequent intervals to compensate for any shift in the slope of the calibration curves over a period of time. Calibration constants have been found to be independent of tunnel pressure and temperature. Zero readings, however, shifted over a considerable range with changes in tunnel temperature. This shift, it has been found, could be correlated with readings of thermocouples fixed to the base of the strain-gage windings. All readings were corrected for this zero shift. Lift-drag interaction, a result of a small component of the lift acting upon the drag gage due to the strain-gage cantilever springs deflecting under load, which has been found to be a necessary drag correction at high values of lift, was found to be negligible through the limits of this investigation. The possible existence of nonrepeating errors was refuted by the excellent agreement of the results of repeated runs.

The initial angle of attack of the model was measured under static conditions before each run by means of a height gage and a leveled surface plate inside the test section. During the run aerodynamic loads caused deflection of the sting in direct proportion to the lift load involved. All angles of attack were corrected for this deflection. The deflections were calculated from the measured lift values, using constants previously determined by loading the model statically at its center of pressure. Some uncertainty exists as to the magnitude of error involved in determining the angle of attack by this method as the vibration of the model and support during testing was of sufficient amplitude and frequency to prevent any accurate check by optical means.

Shrouding, provided the balance is sealed to prevent the flow of air within it, serves to eliminate all aerodynamic forces on the sting. Deflection of the sting under high lift loads, however, caused fouling against the shroud at angles of attack greater than 4°, thus limiting the use of a shroud. Tares due to aerodynamic forces on the sting were determined from results of a series of runs of the model through the -2° to 4° angle-of-attack range with and without a shroud which was mounted on the nosecap of the balance housing and enclosed the sting to within 1/32 inch of the base of the model. The lift and drag tares for angles of attack greater than 4° then were determined by extrapolation of the differences

determined from the low angle-of-attack runs. All drag data in this report are corrected for aerodynamic forces on the sting. The lift tare was found to be negligible, so no corrections were applied. The model was pivoted at the design center of gravity and the pitching moment was measured on a strain gage situated inside of the model, thereby eliminating the necessity of determining force tares for moment. No attempt was made to correct for the unknown effects of support interference.

The results, determined from the measured lift, drag, and pitching moment, have been corrected for the effects of tunnel-wall interference by the method of reference 7.

The data were unaffected by choking phenomena at angles of attack less than 6°, as choking at these lower angles was caused by the balance housing which was situated well behind the model. Data presented for choking Mach numbers at higher angles of attack are considered to be of doubtful value and are indicated by broken lines.

DISCUSSION OF RESULTS

Inasmuch as the primary purpose of the investigation was to determine the accuracy with which full-scale flight characteristics can be predicted from high-speed wind-tunnel tests of small-scale models, the high-speed aerodynamic characteristics obtained will be analyzed in conjunction with 1/3-scale model high-speed wind-tunnel results (reference 4) and full-scale flight results. Results of tests using various devices to increase the effective Reynolds number of the tests will be discussed in conjunction with an analysis of the observed flow pattern in the model wing boundary layer. Following this analysis, differences in the results obtained for the various scale models will be compared with Ferri's findings on Reynolds number effects at high speeds (reference 2). The longitudinal stability and control characteristics of the 1/78-scale model will be analyzed in an effort to indicate some of the longitudinal control difficulties to be encountered by conventional aircraft when flying at high subsonic speeds.

High-Speed Aerodynamic Characteristics

In figures 8, 9, and 10, the drag and lift forces and pitching moments of the 1/78-scale model are presented in coefficient form as functions of Mach number and angle of attack. Model-drag coefficients as functions of Mach number are presented in figure 11 for lift coefficients from 0 to 0.4. A comparison of the drag

coefficients for the airplane as measured in flight, for the complete 1/3-scale model as measured in the Ames 16-foot high-speed wind tunnel, and for the 1/78-scale model as measured in the Ames 1- by $3\frac{1}{2}$-foot high-speed wind tunnel is presented in figure 12. The wind-tunnel results are plotted for constant lift coefficient, and flight results are presented for various normal force coefficients as indicated. For the low angles of attack represented by the indicated lift coefficients, the difference between lift coefficient and normal-force coefficient is negligible. Results indicate lower drag-divergence Mach numbers for the 1/78-scale model than for either 1/3-scale or full-scale models; also, the rate of drag rise past the force break is appreciably less than for the larger scale models.

The lift-coefficient variation with Mach number at constant angle of attack for the 1/78-scale model is illustrated in figure 13. Although these model results exhibit lift-coefficient trends with Mach number which are very similar to the 1/3-scale and full-scale results, the magnitude of the lift coefficient at a given angle of attack for the 1/78-scale model is at variance with the larger scale results throughout the Mach number range of the tests, as demonstrated in figure 14. Throughout the entire angle-of-attack range investigated, lift divergence occurs at a lower Mach number for the 1/78-scale model than for either the 1/3-scale model or the full-scale airplane. The 1/78-scale results exhibit lower lift coefficients throughout the speed range, and a more gradual decrease in lift coefficient with Mach number beyond the force break than do either the 1/3-scale or full-scale results. An increase with Mach number in lift coefficient beyond the minimum value is indicated for all angles of attack of the 1/78-scale results at Mach numbers past the upper limit of the 1/3-scale or full-scale tests.

The variation of the lift-curve slope with Mach number for the 1/78-scale model at the design lift coefficient is in excellent agreement with 1/3-scale results as indicated in figure 15. Also indicated are several values taken from full-scale results which agree favorably with the small-scale results, although the scatter is much greater due to the difficulty involved in obtaining these data under flight conditions. The 1/78-scale results reveal an increase in lift-curve slope beyond a Mach number of 0.9 which occurs beyond the limiting Mach number of the previous investigations.

The angle for zero lift for the 1/78-scale model begins shifting to a positive value approximately 0.1 Mach number before a similar trend begins for the 1/3-scale model with the increase occurring more gradually for the 1/78-scale model than for the larger scale model. (See fig. 16.) The angle for zero lift attains a maximum positive value for the 1/78-scale model at approximately 0.86 Mach number (the limit of the 1/3-scale tests) and thereafter returns to a negative value.

The pitching-moment coefficient variation with Mach number for the 1/78-scale model as a function of lift coefficient is presented in figure 17. A comparison of 1/78-scale, 1/3-scale, and full-scale pitching-moment results is presented in figure 18. The pitching-moment coefficient trend with Mach number is similar for the various configurations up to approximately 0.8 Mach number beyond which a considerable discrepancy exists. The 1/78-scale results do not indicate the diving tendency in the Mach number range of 0.8 to 0.86 apparent from the larger scale results, but, to the contrary, exhibit for lift coefficients above 0.1 a pitch-up tendency which becomes more severe with increasing lift. As seen from figure 18, an abrupt pitch-up motion appeared in full-scale tests only at the limiting Mach number of the tests (approximately 0.85 Mach number). During flight tests of the YP-80A, a sudden pitch-up motion of the airplane occurred at a Mach number of 0.85 as the Mach number was being decreased from 0.866 and resulted in a change in lift coefficient from 0.49 to 0.89 in about 1 second. (See reference 5.) The prematurely occurring nose-up change in balance for the 1/78-scale model is consistent with the previously noted effects of low-scale on the lift and drag characteristics. A diving tendency becomes apparent for the 1/78-scale model beyond a Mach number of 0.90 and increases in severity to the limiting Mach number of the tests.

The pitching-moment coefficient variation with Mach number for the 1/78-scale YP-80A model is qualitatively similar to that for the Bell XS-1 airplane (reference 8) in the transonic-speed region as seen from figure 19. This similarity suggests the possibility that stability and control problems evidenced by the 1/78-scale YP-80A model test results are not peculiar to the specific model tested, but are representative of stability and control problems to be encountered by conventional aircraft when flying in the range of Mach numbers corresponding to those of the present tests.

Scale Effects

In an attempt to effectively increase the scale of the present tests by forcing a local flow over the model wings which would correspond to Reynolds numbers of the order of full-scale flight tests, carborundum was applied successively to the upper surfaces of the model wings at 50 and 20 percent of the wing chord so as to fix transition from laminar flow to turbulent flow at these respective positions. Aerodynamic characteristics were determined for the model in these conditions over the range of test Mach numbers. No significant changes in the principal force and moment characteristics were observed for either model condition, indicating that the carborundum was not effective in fixing transition. In a

further effort to increase the effective Reynolds numbers of the tests by forcing early transition from laminar to turbulent flow, a grid of bars was installed just upstream of the wind-tunnel test section to increase the turbulence of the air stream. Several model tests were made and then repeated with the grid removed. No appreciable changes in the model force characteristics were effected through the increased turbulence.

To determine the nature of the flow within the boundary layer and how it is effected by the carborundum and turbulence grid a liquid-film method for visualizing boundary-layer flows, previously noted under Tests, was used in conjunction with the turbulence grid tests. A strip of carborundum was fixed at the 20-percent-chord station on the upper surface of the left wing of the 1/78-scale model for these tests. Results indicate no significant differences in the flow patterns over the model with and without the turbulence grid. In figure 20 are presented the flow patterns for the 1/78-scale model for 4° angle of attack and 0.6 Mach number as obtained with and without the turbulence grid installed. The carborundum was apparently ineffective inasmuch as the over-all flow pattern on the left wing was little changed from that of the right wing; the only significant difference being an alteration in the flow at the tip.

Referring to the boundary-layer flow photographs of figure 20, a wet region, indicative of low surface shear in the boundary layer, appears as a white area on the model surface; and, conversely, a dry region, indicative of high surface shear in the boundary layer, appears as a black area. The presence of the wet region just aft of the leading edge of the right wing indicated low surface shear in this region and could denote separation of the laminar boundary layer should a sufficiently adverse pressure gradient (decelerated flow) exist there. A tendency to separation of the laminar boundary layer, according to reference 9, could be present at a point near the nose of an airfoil at any moderately high lift coefficient if the Reynolds number is not sufficiently high to make the flow turbulent at that point. An examination of the pressure distribution over an NACA 65_2-215 (a=0.5) airfoil section (reference 10), a section closely related to that of the subject model, for comparable Mach number and angle of attack, however, indicates that a favorable pressure gradient (accelerated flow) exists over the forward portion of the airfoil, thereby precluding the possibility of a tendency to laminar separation. The inconsistency between the pressure gradient, as indicated from the probable pressure distribution and the pressure gradient necessary to support the indicated flow pattern, led to the conclusion that the 1/78-scale model wing section was probably inaccurately machined. A metal casting of the profile of the model wing was made and cut at a specified section to

check the accuracy of the ordinates. The variation of the measured with the intended ordinates is shown in figure 21. The position and magnitude of the maximum thickness is as specified and the profile beyond this point is within the allowable accuracy; therefore, only the portion forward of this position is illustrated. The measured profile was found to have a larger leading-edge radius and, consequently, thicker nose section than has the specified NACA 65_1-213 (a=0.5) low-drag section.

The pressure distribution over the measured profile, presented in figure 22, was calculated by the method of reference 11 and corrected by the Glauert compressibility factor $\sqrt{1-M^2}$. An adverse pressure gradient is seen to exist over the 5- to 15-percent-chord region of the upper surface of the airfoil section. The indicated pressure recovery is not sufficient to support laminar separation, but does support the contention of low surface shear in the boundary layer in this region. Further evidence in support of the flow pattern indicated for the 1/78-scale wing is evident in the favorable pressure gradient existing over the 15- to 25-percent chord region of the upper surface, the effect of the favorable gradient being to speed up the energy-deficient air in the boundary layer close to the surface, thus increasing the surface shear and drying that portion of the wing surface. Aft of the 25-percent chord position the wet area is consistent with a laminar boundary layer subject to an adverse gradient. The dried region in the latter 15-percent of the wing chord indicates that transition to turbulent flow has occurred.

The abnormally long laminar run of the boundary layer indicated by the foregoing analysis is further evident in the fact that the fuselage is wet over the entire length of the model with no indication of turbulent flow even behind the canopy or air intake bulges. Thus it seems likely that the marked differences between the 1/78-scale and full-scale results, as indicated by the results of the present investigation, are due mainly to differences in scale, although the unpredicted modification in the specified airfoil section for the 1/78-scale model may be a contributing factor. The thickening of the forward portion of the wing probably contributed to a lowering of the force divergence velocity and to an increase in the angle of zero lift beyond the critical Mach number for the airfoil section.

The marked differences between 1/78-scale and full-scale results, described in the foregoing sections, are significantly similar to those indicated in Ferri's results of reference 2. Data on an NACA 0015-64 airfoil, obtained in the 1.31- by 1.74-foot high-speed wind tunnel at Guidonia, Italy, at a Reynolds number of about 500,000, are compared with those obtained in the 8.86-foot

diameter high-speed wind tunnel at the Deutsche Versuchsanstalt für Luftfahrt (DVL) in Germany at approximately 6,000,000 Reynolds number. The results from the two tunnels are at variance, especially at high speeds. As illustrated in figure 23, the drag divergence Mach number indicated from the 500,000 Reynolds number results is lower and the rate of drag rise past the critical speed less than indicated from the 6,000,000 Reynolds number results. Also, as illustrated in figure 24, the lift-force break for the low Reynolds number tests occurs at a lower Mach number and is followed by a more gradual decrease in lift than for the high Reynolds number tests. This lack of agreement is attributed by Ferri to the difference in testing technique and the proportions of the testing systems. From the analysis of the results of the present investigation, however, it would appear that this lack of agreement is more probably due to differences in scale.

Longitudinal Stability

Below a Mach number of 0.84, the 1/78-scale model of the YP-80A airplane exhibits adequate longitudinal stability with little variation throughout the lift-coefficient range of the test. (See fig. 25.) Beyond this Mach number a gradual decrease in static stability is evident up to a Mach number of about 0.90 with the most pronounced change occurring at high lift coefficients. Beyond this Mach number, however, a sudden increase in longitudinal stability becomes apparent. The diving tendency, shown to exist beyond a Mach number of 0.90, when accompanied by this rapid increase in longitudinal stability, presents a serious longitudinal control problem.

The 1/78-scale model with the tail removed exhibits a gradual decrease in static longitudinal instability with increasing speed up to a Mach number of about 0.80. (See fig. 26.) Beyond this Mach number, a reversal of longitudinal instability is indicated between lift coefficients of 0.1 and 0.4 up to the limiting Mach number of the test. This reversal of instability is evident from 1/3-scale tests (reference 4) only at 0.85 Mach number, the limit of the tests. At a Mach number of about 0.95, however, the 1/78-scale model without tail is stable throughout the lift-coefficient range investigated.

It has been found from an Ames 16-foot high-speed wind-tunnel investigation of a model tail plane with 0° and 45° sweepback (unpublished data on file at the laboratory) that Mach number effect on stabilizer effectiveness can be alleviated by sweepback. Therefore, in an effort to improve the longitudinal-stability characteristics at supercritical speeds, the leading edges of the horizontal- and vertical-tail surfaces of the 1/78-scale model were swept back 45°.

The area of the horizontal tail and elevator were maintained effectively the same as those of the original surfaces, while the vertical-tail area was increased some 30-percent. Results from tests of the swept-back-tail version of the subject model (fig. 27) indicate that, below a Mach number of about 0.83, the swept-back-tail model exhibits a lesser degree of static longitudinal stability than does the conventional configuration. Beyond a Mach number of 0.83, the swept-back-tail configuration tends to become increasingly stable with increasing Mach number to the limits of the test except for a small region of instability at a Mach number of about 0.93 for lift coefficients of 0.4 to 0.5. This region of instability at high lift coefficients occurs for the conventional configuration at approximately the same Mach number as for the swept-tail version.

In general, the static longitudinal-stability characteristics of the 1/78-scale model of the YP-80A airplane were improved by sweeping back the leading edges of the horizontal- and vertical-tail surfaces in that the region of instability at moderate lift coefficients in the Mach number range of 0.83 to 0.90 was eliminated.

Longitudinal-Control Effectiveness

Increments in pitching-moment coefficient produced by various elevator deflections are presented in figure 28 for the 1/78-scale model of the subject airplane. The marked ineffectiveness of the elevators for the -4° deflection for low lift coefficients was presumably due to the effects of low Reynolds number inasmuch as no comparable ineffectiveness was evident from the 1/3-scale model test results of reference 4. An elevator deflection of -8° produced a pitching-moment coefficient increment of about 0.140 at a Mach number of about 0.70, for low-lift coefficients, with very little loss in effectiveness with increasing Mach number. For comparable Mach number and lift coefficient, 1/3-scale tests indicate a pitching-moment coefficient increment of about 0.08 for a -8° elevator deflection with but a slight decrease in effectiveness at higher Mach numbers. At a lift coefficient of 0.4, for the 1/78-scale model, elevator effectiveness for the -8° deflection dropped off rapidly above a Mach number of 0.80, increasing slightly again at a Mach number of 0.93.

CONCLUDING REMARKS

A comparison of 1/78-scale test results with those obtained at higher Reynolds numbers disclosed marked differences between 1/78-scale and full-scale aerodynamic characteristics. Most significant among indicated differences is the premature occurrence of the lift and drag force breaks for the 1/78-scale model. Less prominent,

but none the less important, is the marked lessening in severity of the lift loss and the reduction in the rate of drag rise after the force breaks. An early increase in angle of zero lift is evident for the 1/78-scale model, while the variation in lift-curve slope with Mach number is in excellent agreement with the higher Reynolds number results. Local boundary-layer flows over the model wing, indicated by the liquid-film tests and supported by the calculated pressure distribution, revealed a very long laminar run of the boundary layer over the wing of the 1/78-scale model which was consistent with the low scale of the tests.

The static-longitudinal stability of the 1/78-scale model, above a Mach number of about 0.81, gradually decreases with increasing speed up to a Mach number of 0.90. Beyond this speed a very severe diving tendency is apparent accompanied by a sudden increase in static longitudinal stability. Sweeping back the horizontal and vertical-tail surfaces of the 1/78-scale model effectively eliminated the region of longitudinal instability at moderately high-lift coefficients in the Mach number range of 0.83 to 0.90.

Longitudinal-control tests for the conventional 1/78-scale model of the YP-80A airplane showed marked ineffectiveness of the -4° elevator deflection attributable, apparently, to the small scale of the model. The -8° elevator deflection remained effective throughout the Mach number range of the tests for low-lift coefficients. For lift coefficients near 0.4, however, a rapid loss in effectiveness was evident beyond a Mach number of 0.81 with a slight gain in effectiveness apparent at a Mach number of 0.93. As in 1/3-scale test results, no significant loss in elevator effectiveness with Mach number is evident below 0.81 Mach number throughout the lift-coefficient range of the tests.

Although trends in lift and drag forces and stability and control characteristics of an airplane can be predicted from small-scale high-speed wind-tunnel tests, differences with full-scale flight characteristics can be expected because of Reynolds number effects.

Ames Aeronautical Laboratory,
National Advisory Committee for Aeronautics,
Moffett Field, Calif.

APPENDIX

THE PRINCIPAL DIMENSIONS OF A 1/78-SCALE MODEL OF THE LOCKHEED YP-80A AIRPLANE

Wing

Span	6 inches
Area	5.61 square inches
M. A. C.	1.034 inches
Root section	NACA 65_1-213, a = 0.5
Tip section	NACA 65_1-213, a = 0.5
Dihedral	3°40'
Root incidence	1°
Tip incidence	$-\frac{1}{2}$°
Taper ratio (tip chord/root chord)	0.380

Horizontal tail

Span	2.396 inches
Area (total)	1.03 square inches
Dihedral	0°
Section	NACA 65-010
Incidence	$1\frac{1}{2}$°
Taper ratio (tip chord/root chord)	0.364
Tail length (25 percent of the M.A.C. to the elevator hinge line)	2.530 inches

Elevator area aft of hinge line 0.206 square inch

Vertical tail

Span (height above fuselage reference line)	1.218 inches
Area (total)	0.53 square inch
Section	NACA 65-010
Incidence	0°
Taper ratio (tip chord/root chord)	0.400

Dimensions for swept-back tail:

Horizontal tail

Sweepback (leading edge)	45°
Dihedral	0°
Section	NACA 65-010
Span	2.336 inches
Area	1.209 square inches
Incidence	0°
Taper ratio (tip chord/root chord)	0.411

Vertical tail

Sweepback (leading edge)	45°
Span (height above fuselage reference line)	1.400 inches
Area	0.953 square inch
Incidence	0°
Taper ratio (tip chord/root chord)	0.409

REFERENCES

1. Quinn, John H., and Tucker, Warren A.: Scale and Turbulence Effects on the Lift and Drag Characteristics of the NACA 65_3-418, a = 1.0 Airfoil Section. NACA ACR No. L4H11, 1944.

2. Ferri, Antonio: Completed Tabulation in the United States of Tests of 24 Airfoils at High Mach Numbers (derived from interrupted work at Guidonia, Italy in the 1.31- by 1.74-foot high-speed tunnel). NACA ACR No. L5E21, 1945.

3. Spreiter, John R., and Steffen, Paul J.: Effect of Mach and Reynolds Numbers on Maximum Lift Coefficient. NACA TN No. 1044, 1946.

4. Cleary, Joseph W., and Gray, Lyle J.: High-Speed Wind-Tunnel Tests of a Model Pursuit Airplane and Correlation with Flight Test Results. NACA RM No. A7I16, 1947.

5. Brown, Harvey H., Rolls, L. Stewart, and Clousing, Lawrence A.: An Analysis of Longitudinal-Control Problems Encountered in Flight at Transonic Speeds With a Jet-Propelled Airplane. NACA RM No. A7G03, 1947.

6. Vincenti, Walter G., Nielsen, Jack N., and Matteson, Frederick H.: Investigation of Wing Characteristics at a Mach Number of 1.53. I - Triangular Wing of Aspect Ratio 2. NACA RM No. A7I10, 1947.

7. Thom, A.: Blockage Corrections in a Closed High-Speed Tunnel. R.& M. No. 2033, British A.R.C. 1943.

8. Mattson, Axel T.: Force and Longitudinal Control Characteristics of a 1/16-Scale Model of the Bell XS-1 Transonic Research Airplane at High Mach Numbers. NACA RM No. L7A03, 1947.

9. Jacobs, Eastman N., and Sherman, Albert: Airfoil Section Characteristics as Affected by Variations of the Reynolds Number. NACA Rep. No. 586, 1937.

10. Graham, Donald J., Nitzberg, Gerald E. and Olson, Robert N.: A Systematic Investigation of Pressure Distributions at High Speeds Over Five Representative NACA Low-Drag and Conventional Airfoil Sections. NACA RM No. A7B04, 1947.

11. Theodorsen, Theodore: Theory of Wing Sections of Arbitrary Shape. NACA Rep. No. 411, 1931.

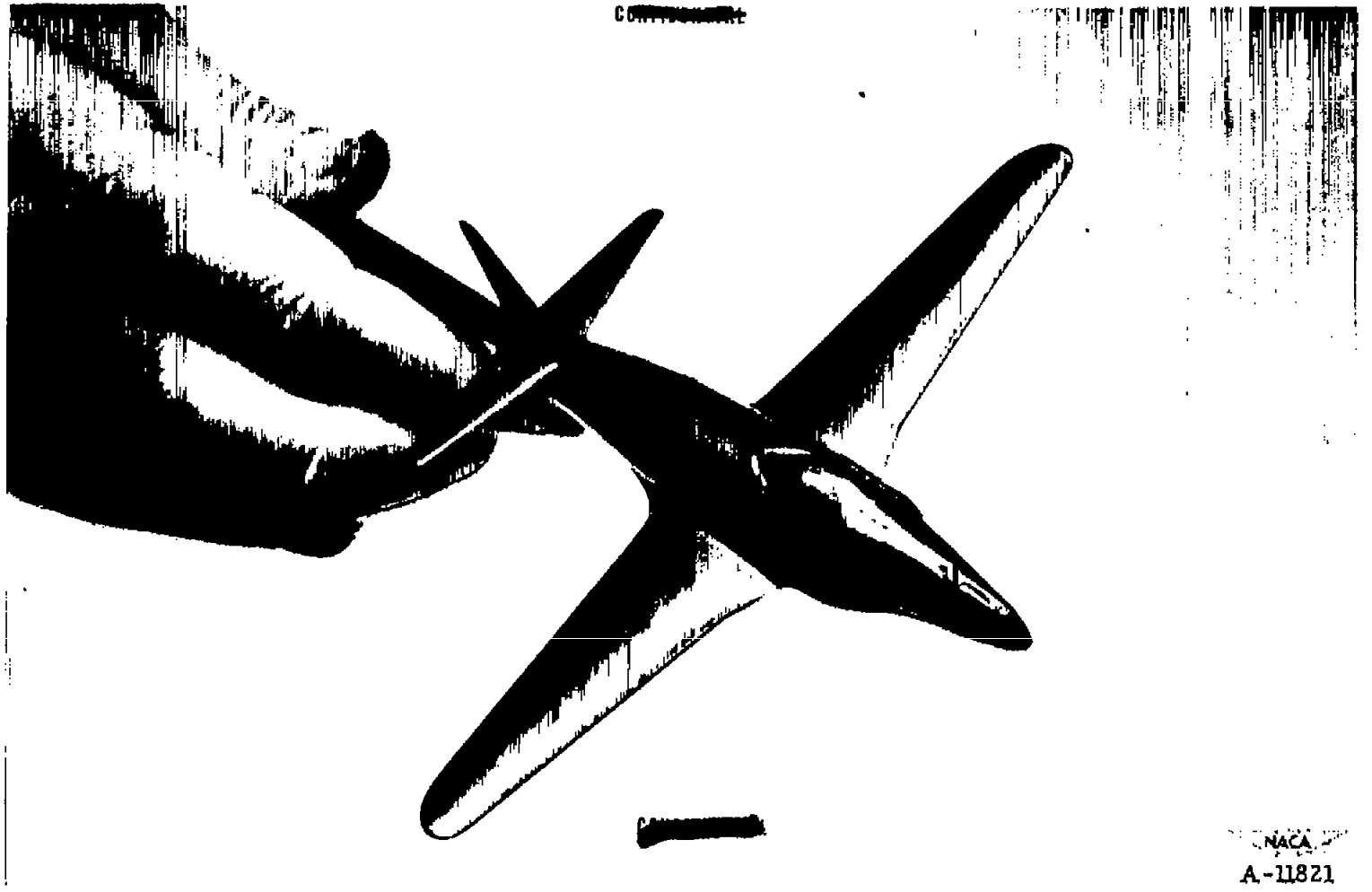

Figure 1.- The 1/78-scale model of the YP-80A airplane (sting mounted).

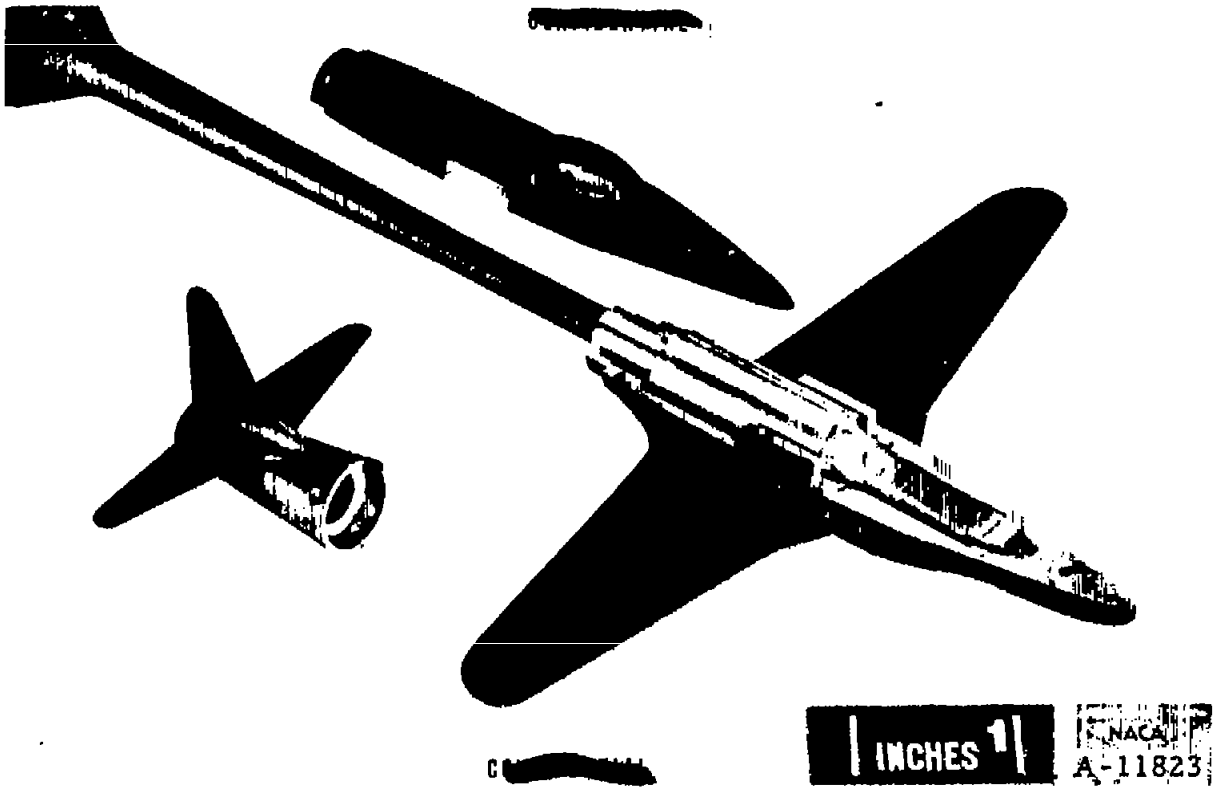

Figure 2.– Exploded view of 1/78-scale model showing split construction and internal pitching-moment strain gage.

NACA
A-11807

Figure 3.- Schematic drawing of the 1/78-scale YP-80A model showing the sting mount and pitching-moment strain-gage installation.

Figure 4.- Tail assemblies used in the 1/78-scale YP-80A model tests.

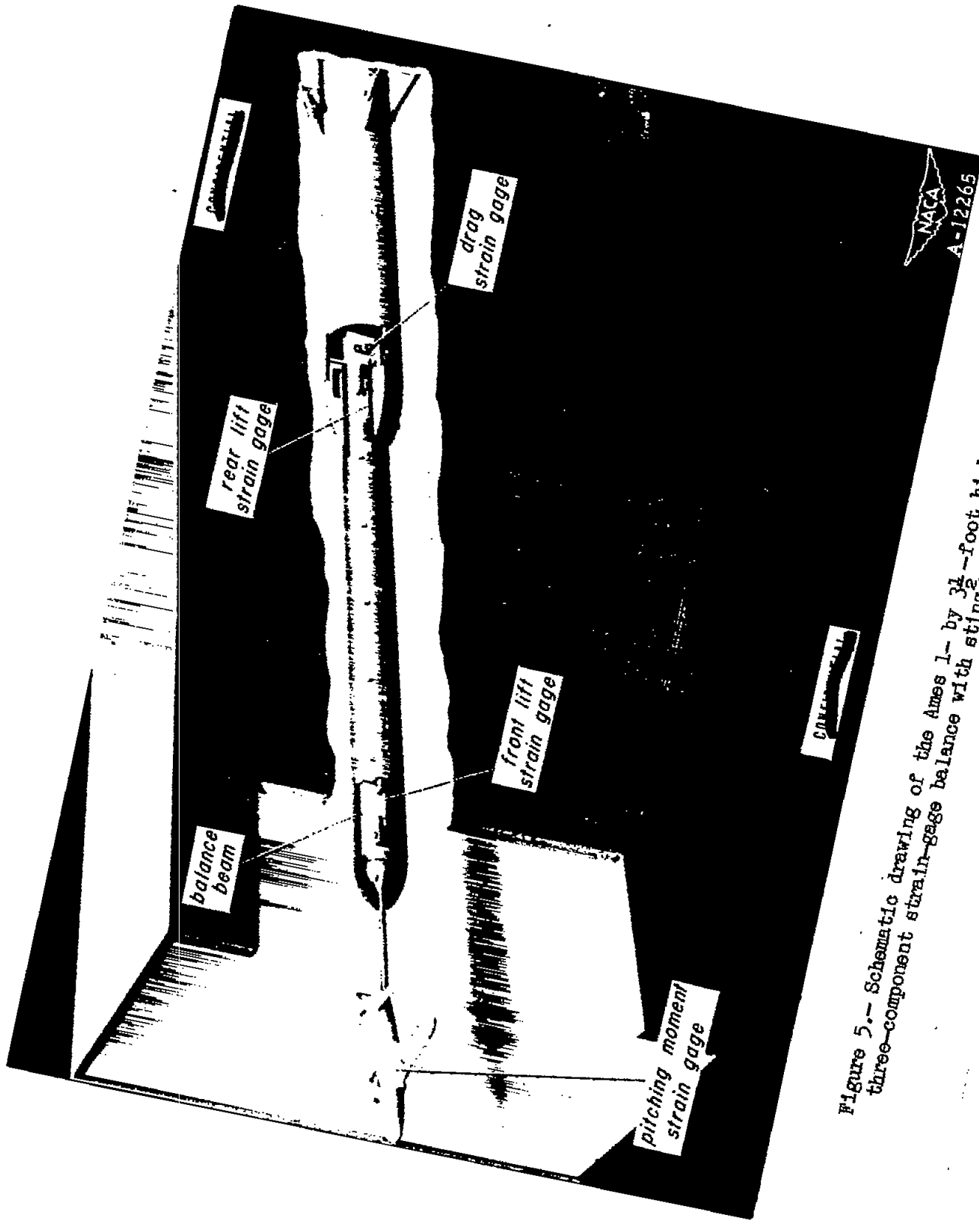

Figure 5.- Schematic drawing of the Ames 1- by 3½-foot high-speed wind-tunnel three-component strain-gage balance with sting-mounted model.

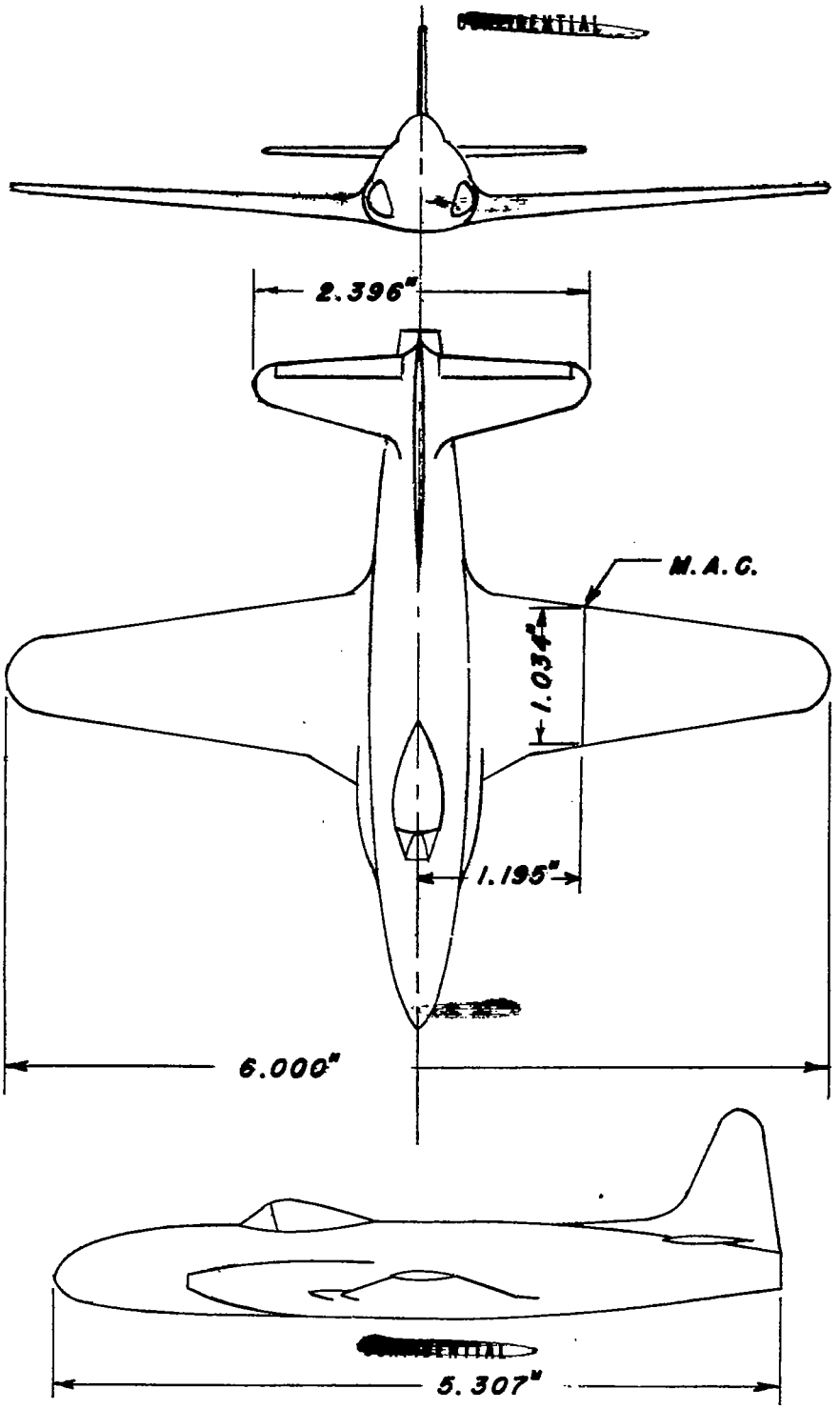

Figure 6.- Three-view drawing of the 1/78-scale model of the YP-80A airplane.

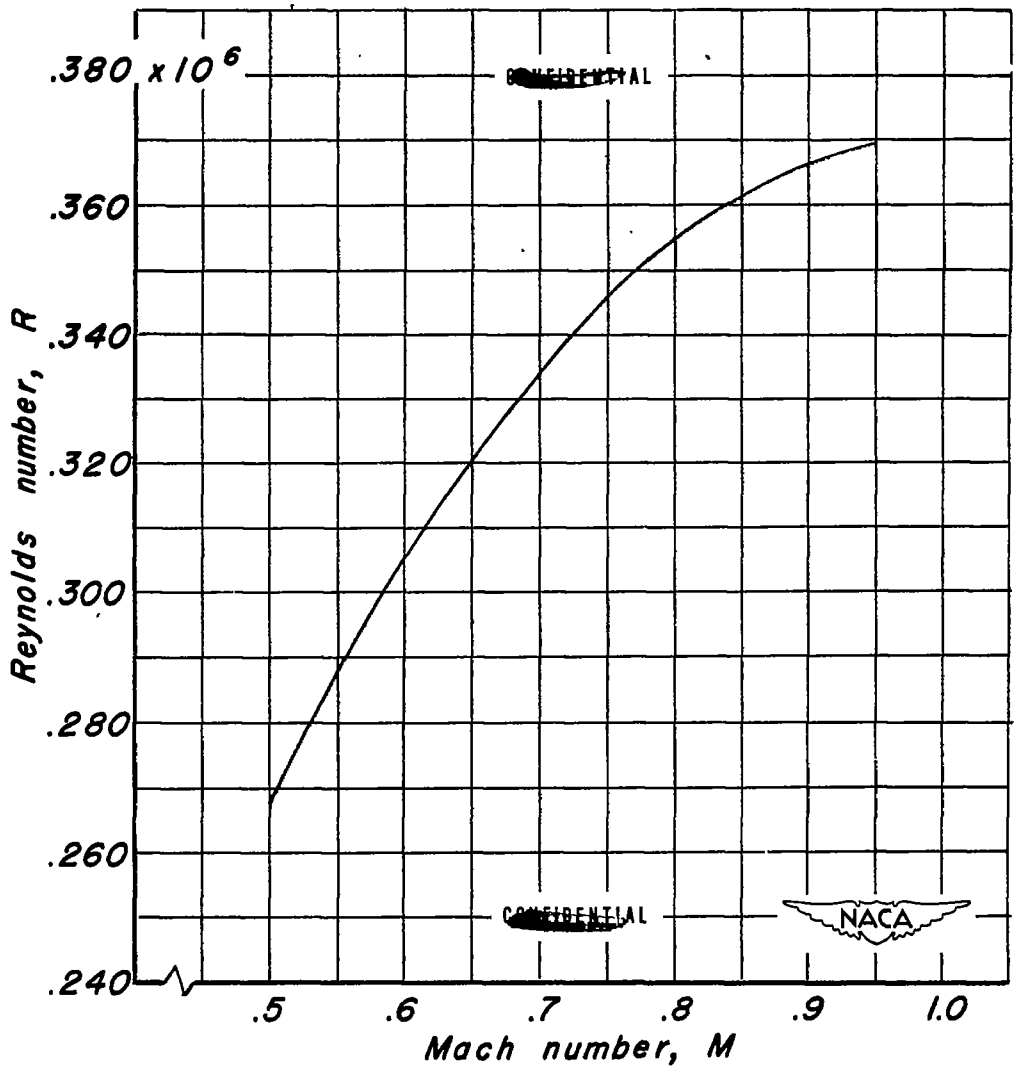

Figure 7.- The variation of Reynolds number with Mach number for the 1/78-scale model of the YP-80A airplane in the Ames 1- by 3½- foot high-speed wind tunnel.

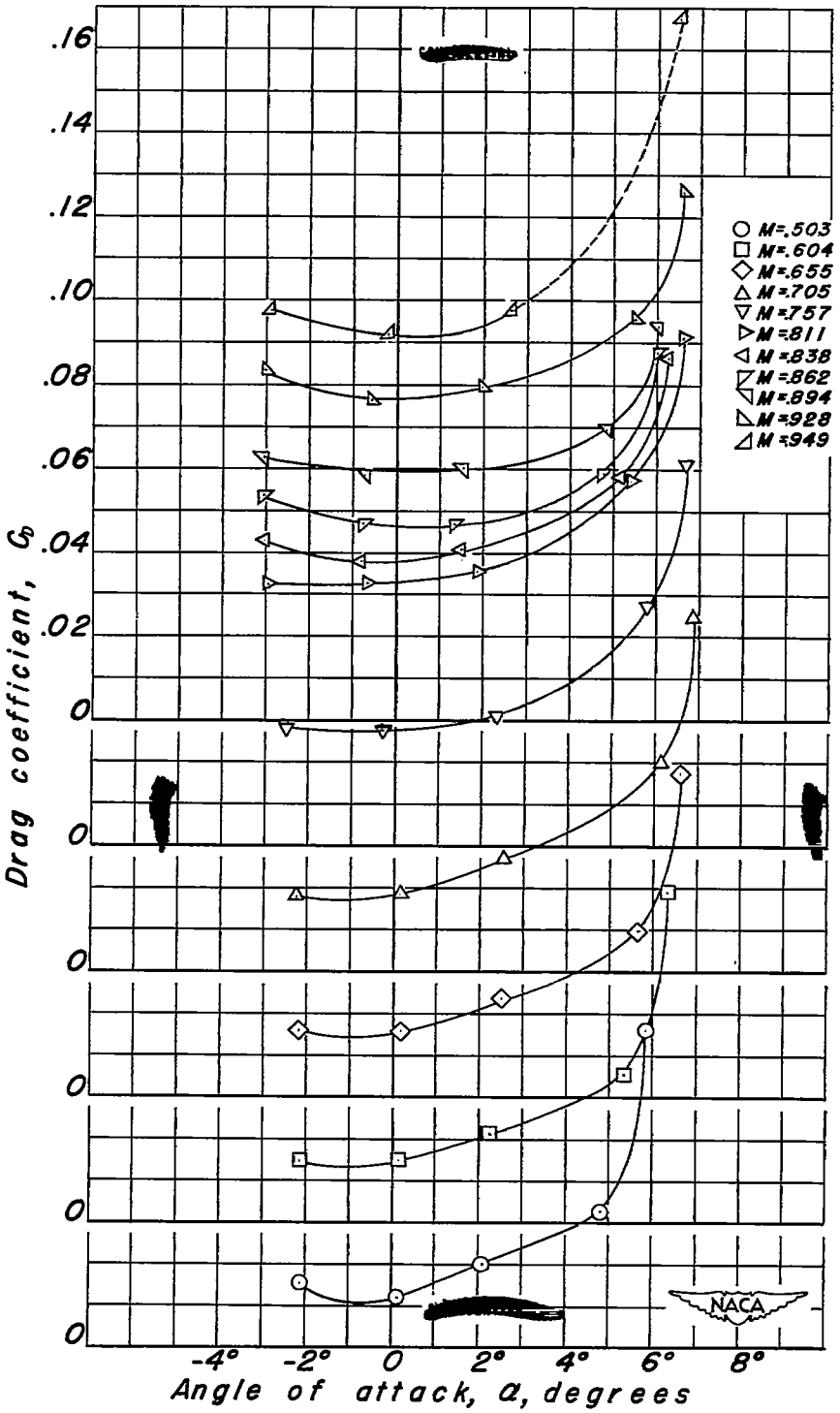

Figure 8.- Variation of drag coefficient with angle of attack for the 1/78-scale model of the YP-80A airplane.

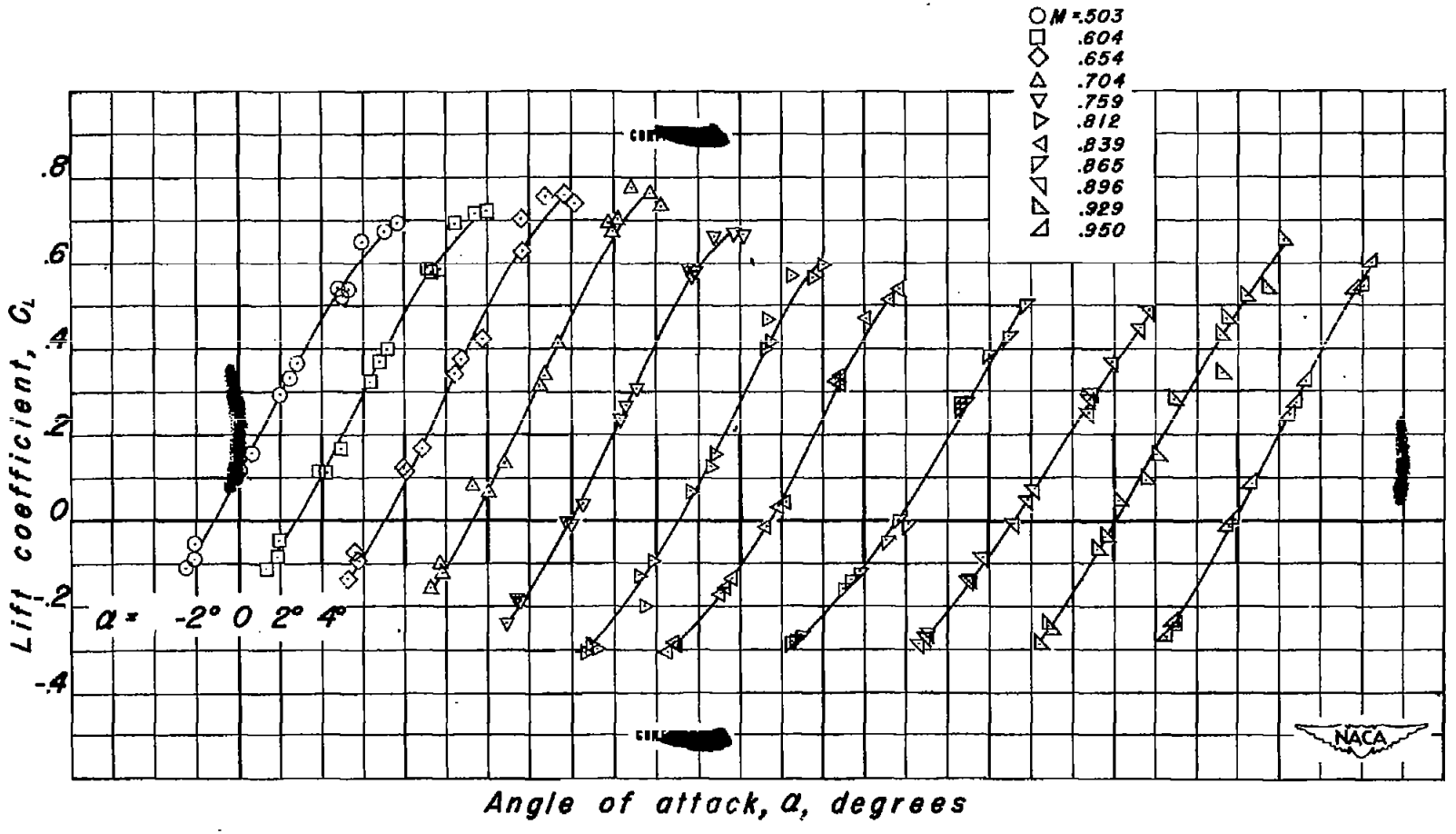

Figure 9.-Variation of lift coefficient with angle of attack for the 1/78-scale model of the YP-80A airplane.

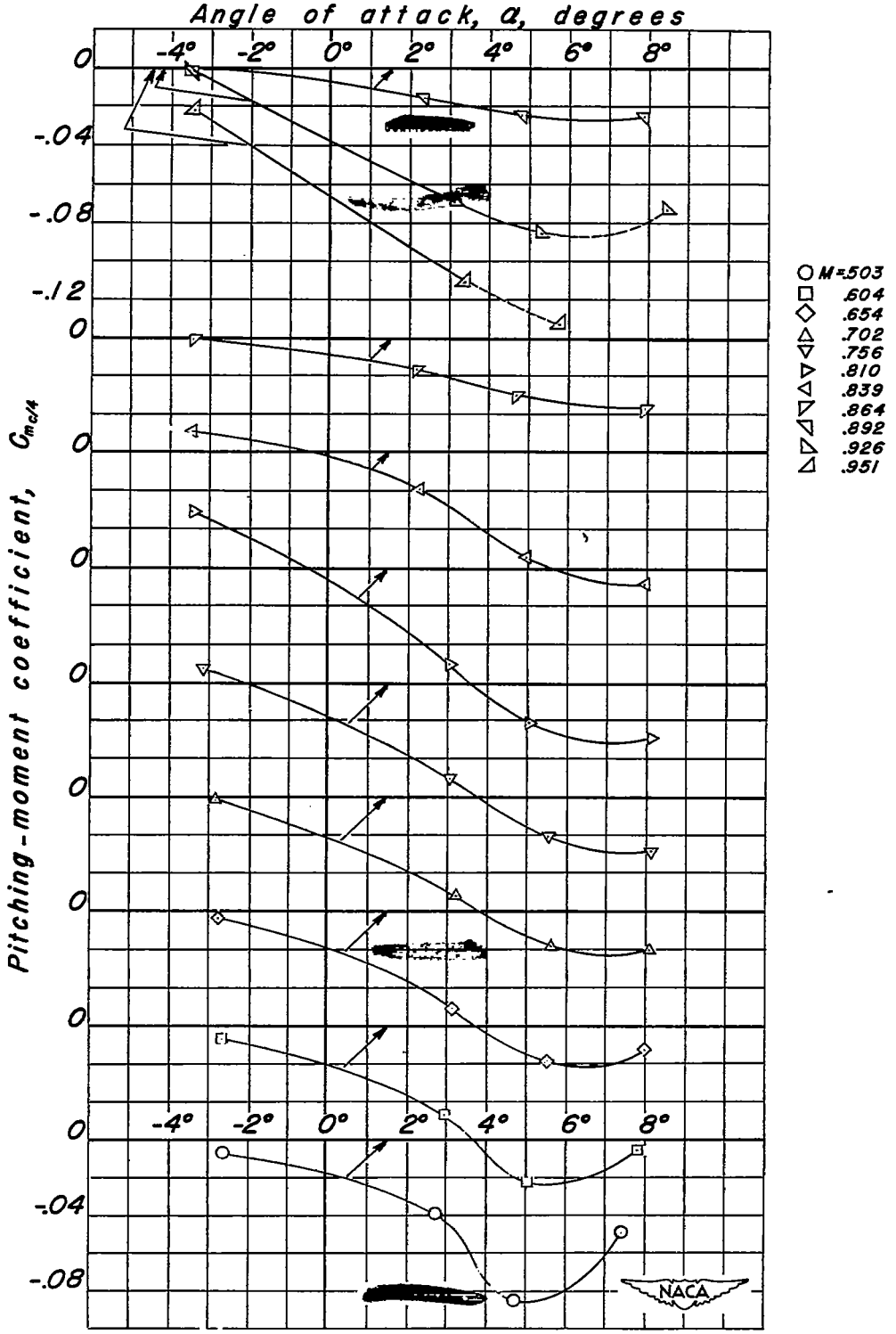

Figure 10.- Variation of the pitching-moment coefficient with angle of attack for the 1/78-scale model of the YP-80A airplane.

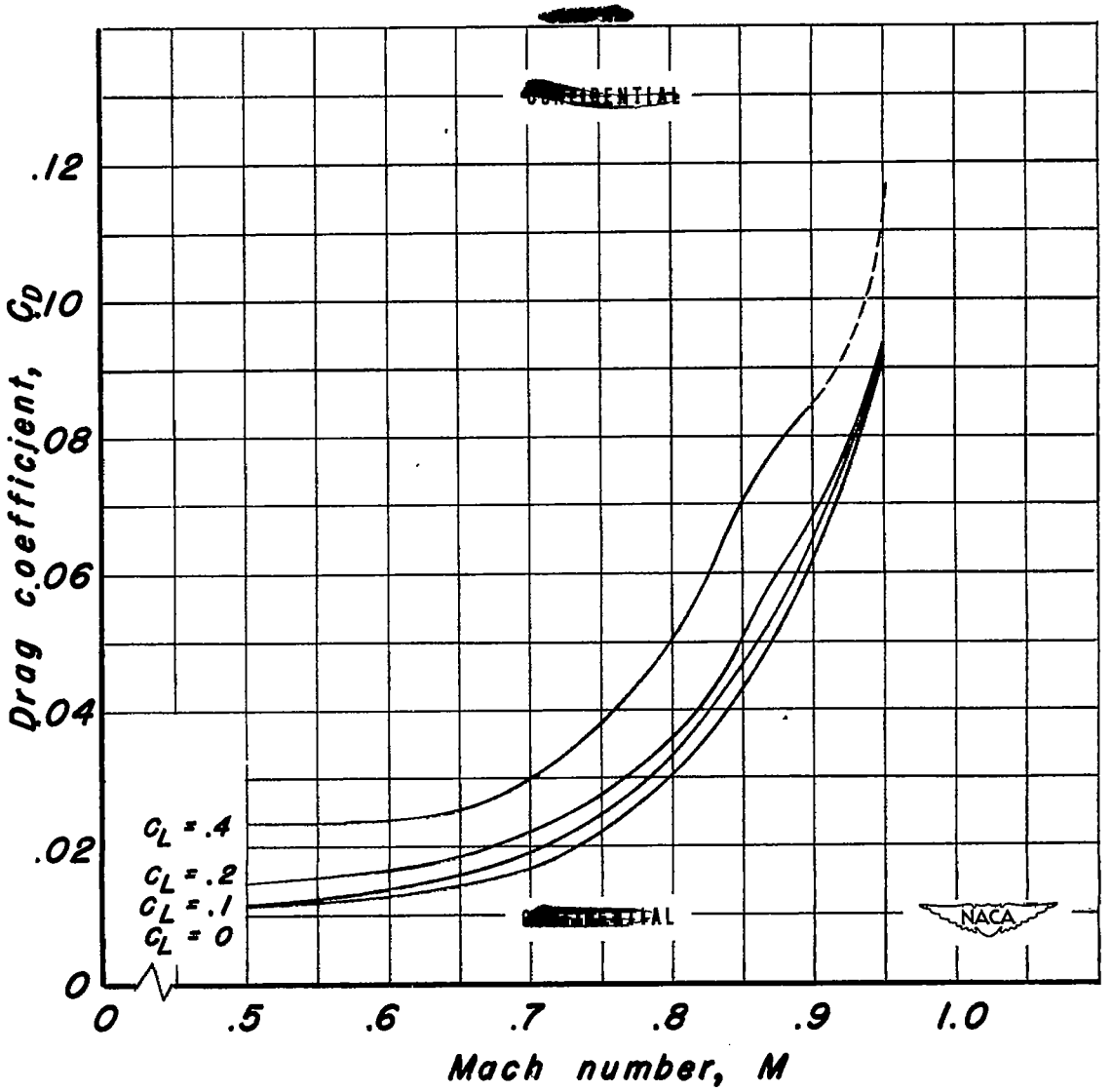

Figure 11.- Variation of drag coefficient with Mach number for the 1/78-scale model of the YP-80A airplane.

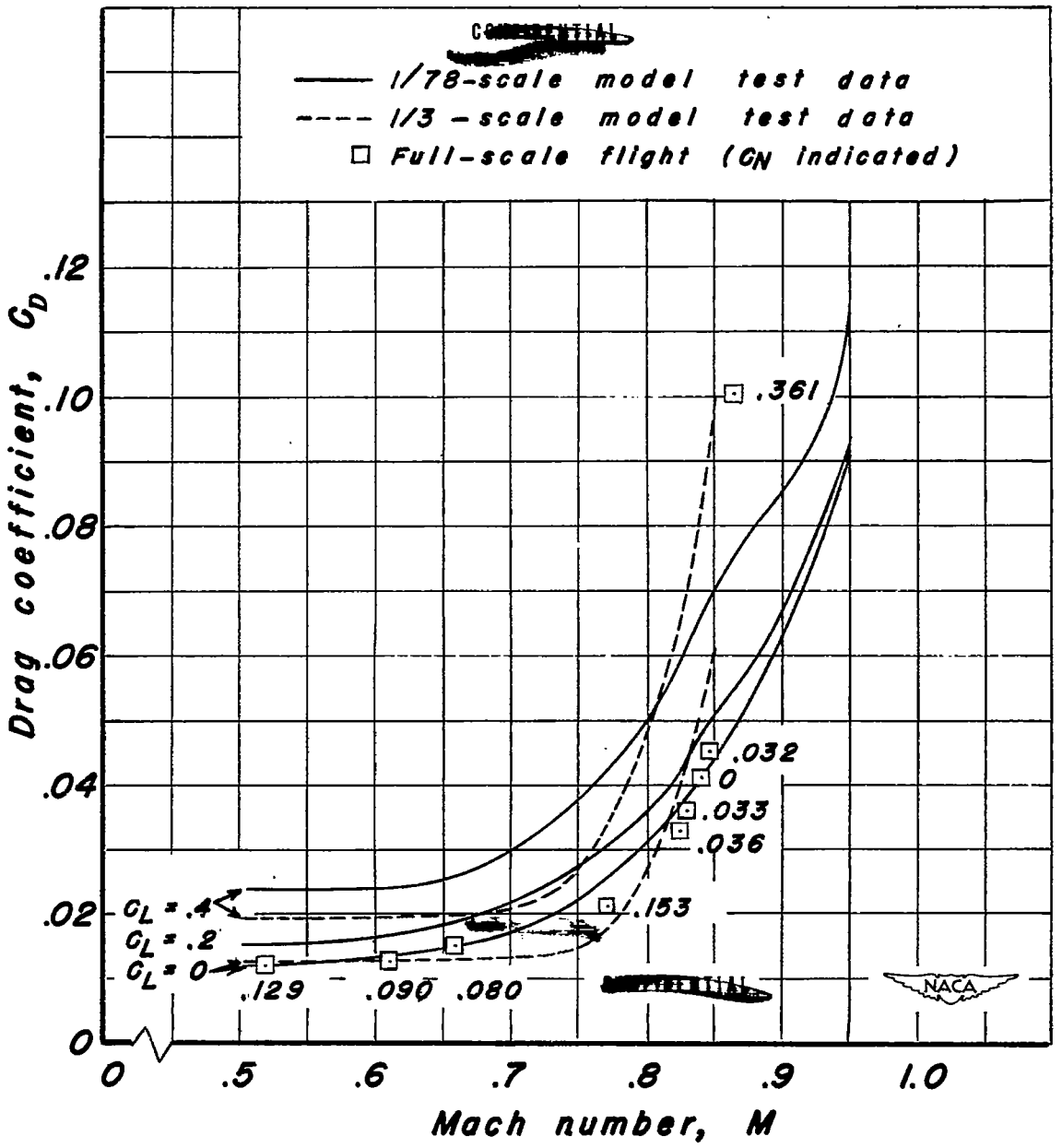

Figure 12.- Comparison of variation of drag coefficient with Mach number for the 1/78-scale model of the YP-80A with results of flight tests of the YP-80A airplane and wind-tunnel tests of a 1/3-scale YP-80A model.

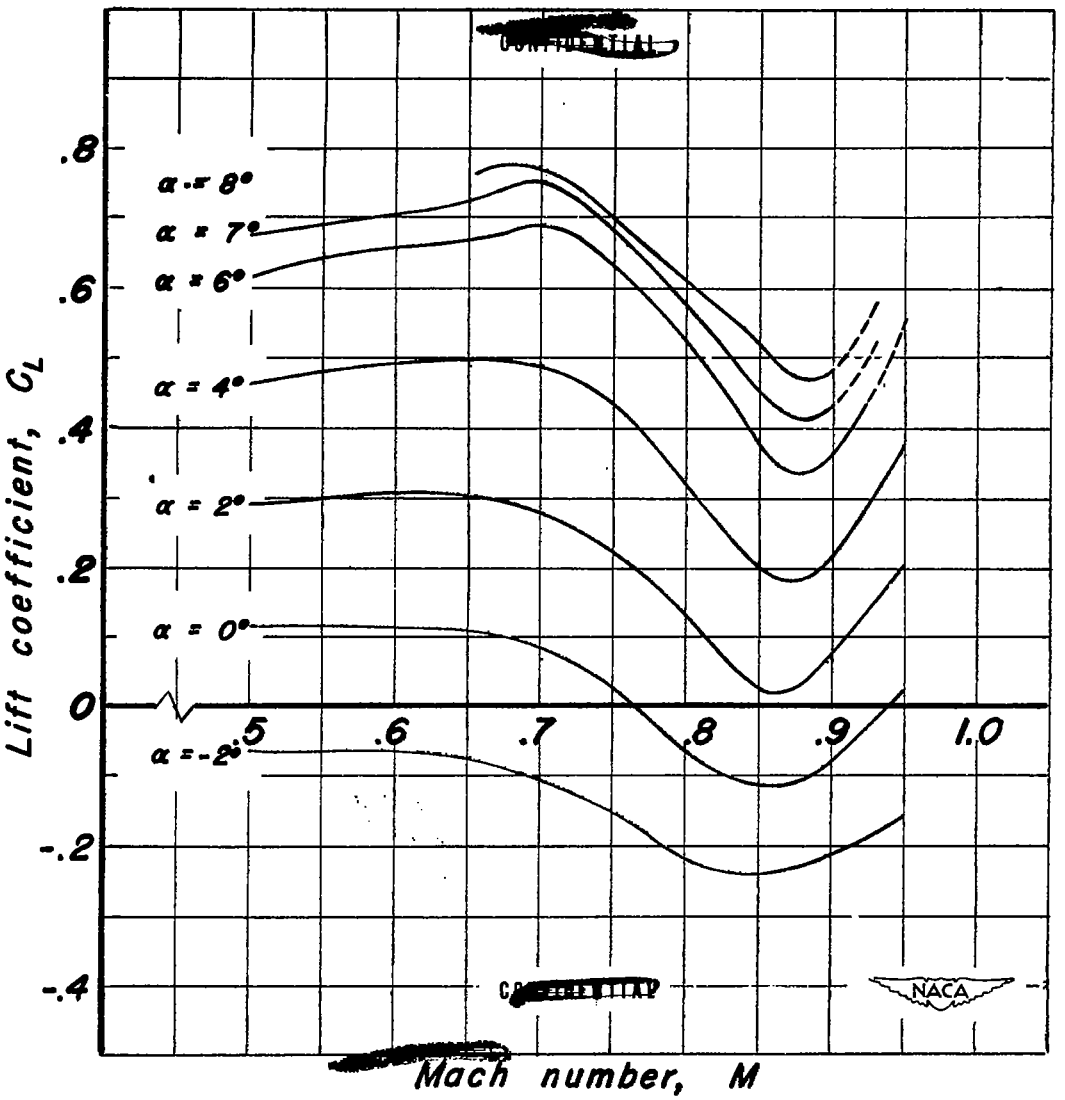

Figure 13.- Variation of lift coefficient with Mach number for the 1/78-scale model of the YP-80A airplane.

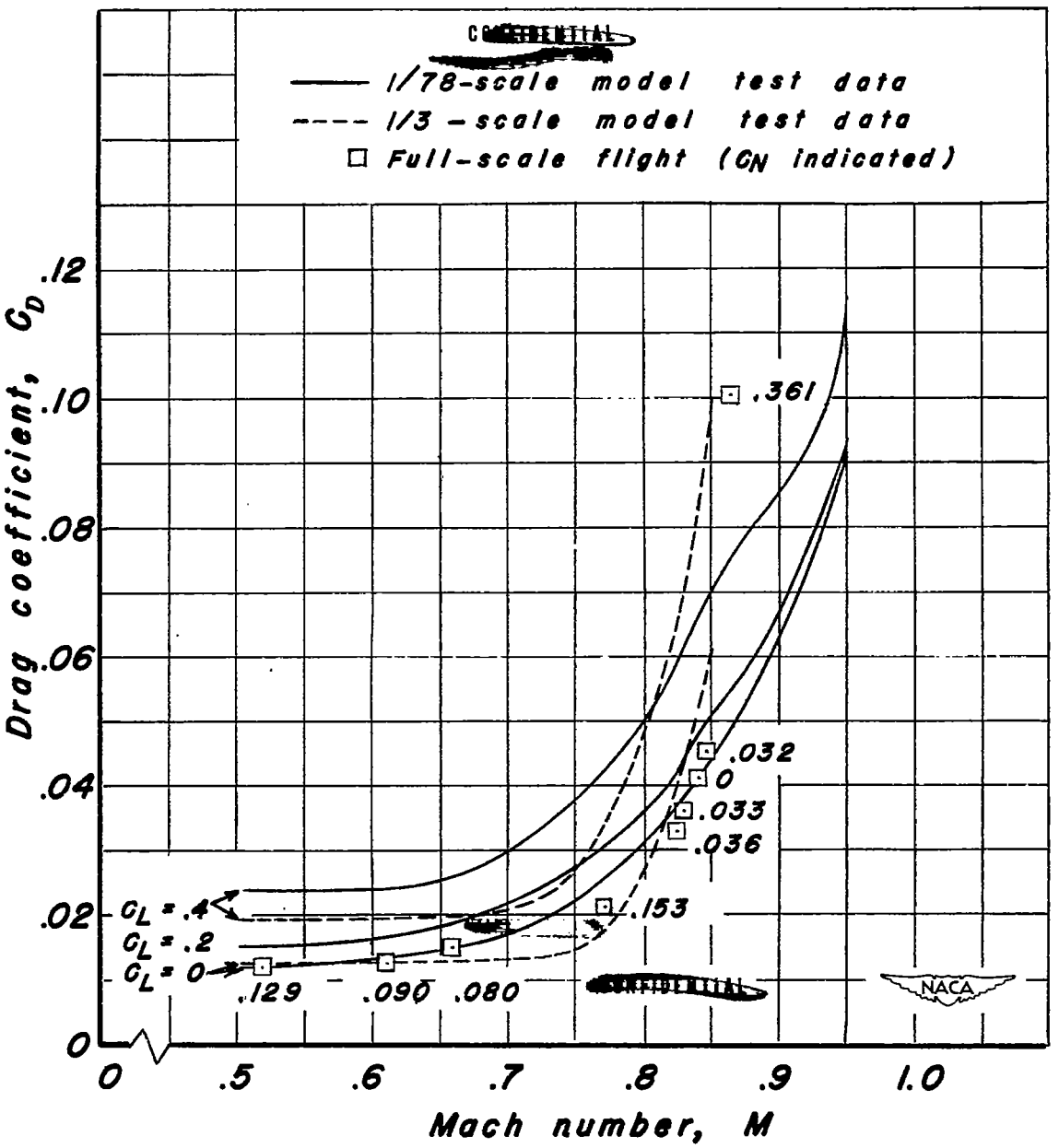

Figure 12.- Comparison of variation of drag coefficient with Mach number for the 1/78-scale model of the YP-80A with results of flight tests of the YP-80A airplane and wind-tunnel tests of a 1/3-scale YP-80A model.

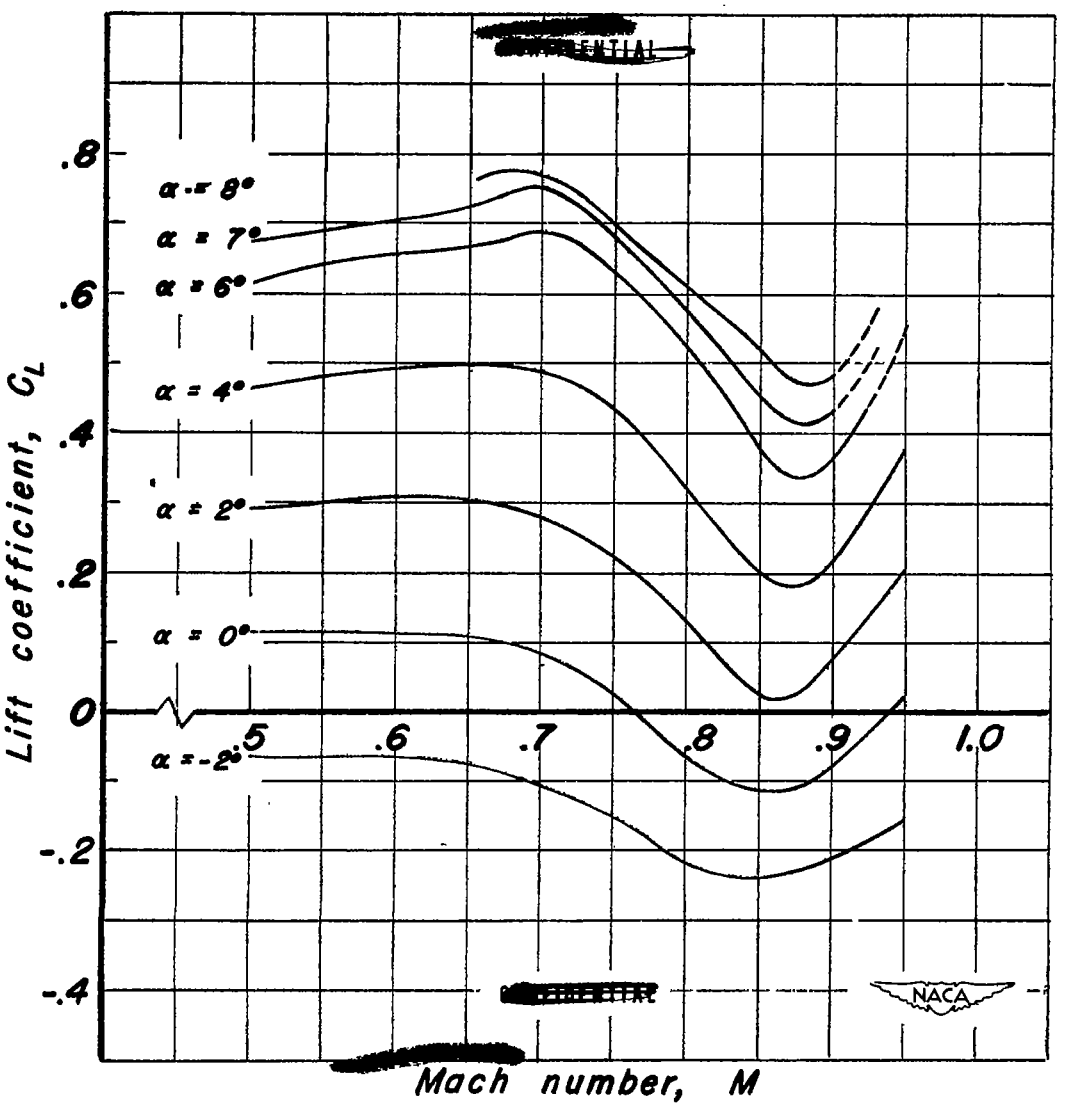

Figure 13.- Variation of lift coefficient with Mach number for the 1/78-scale model of the YP-80A airplane.

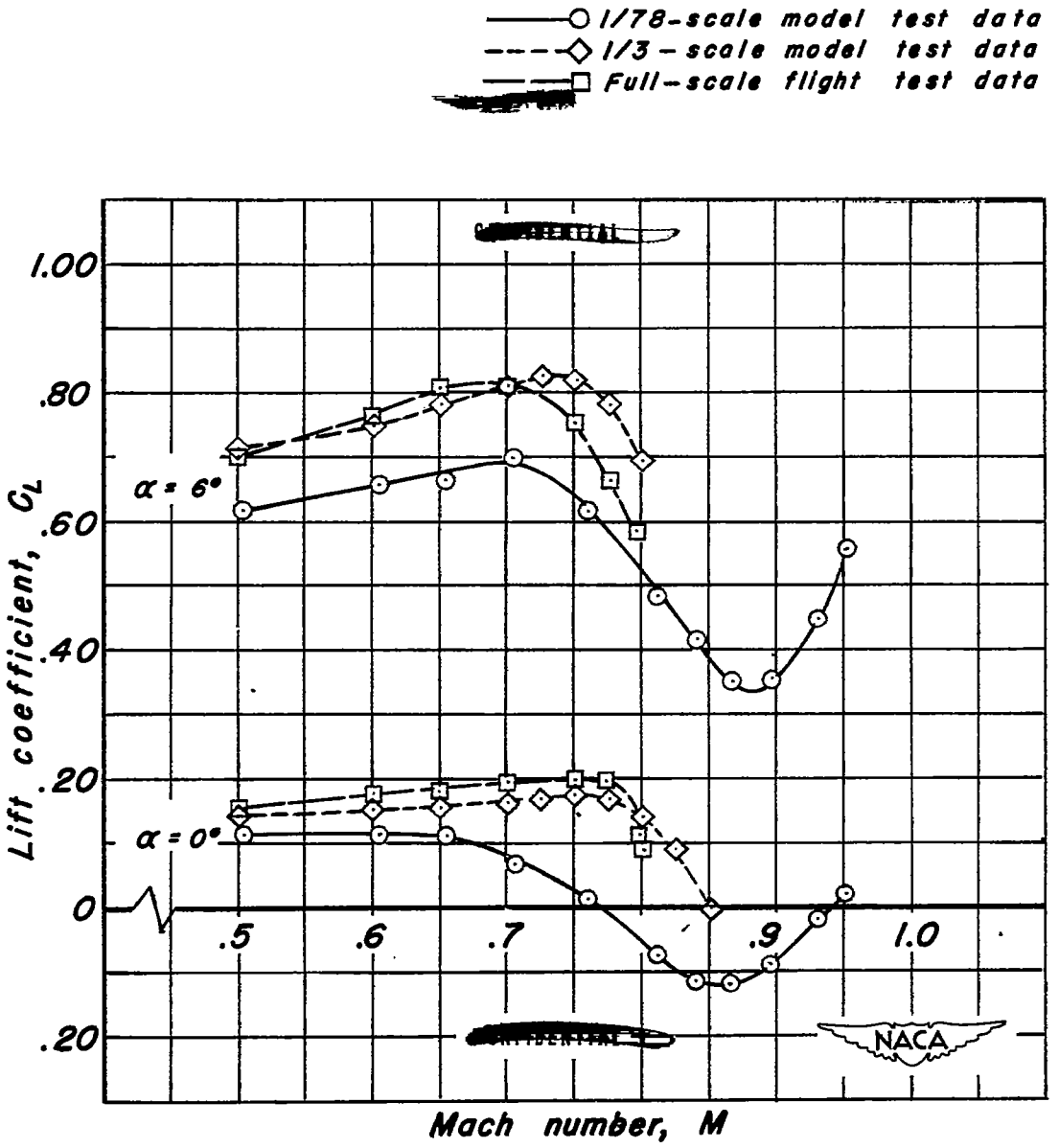

Figure 14.- Comparison of variation of lift coefficient with Mach number for the 1/78-scale model of the YP-80A with results of flight tests of the YP-80A airplane and wind-tunnel tests of a 1/3-scale model of the YP-80A.

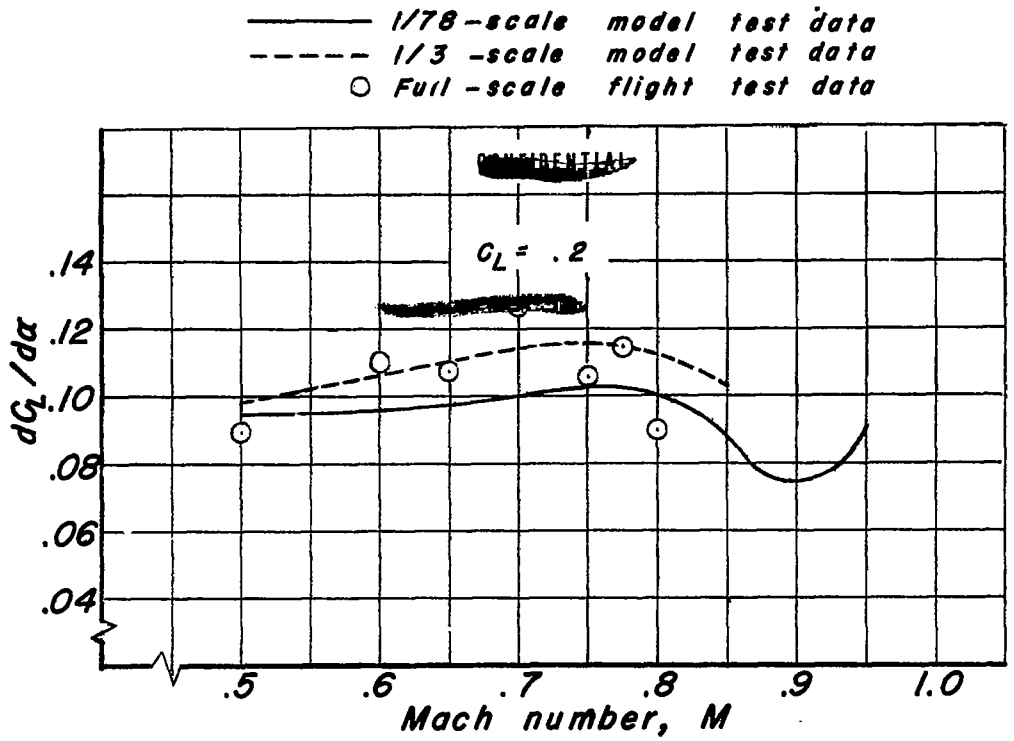

Figure 15.-Comparison of variation of lift-curve slope with Mach number for the 1/78-scale model of the YP-80A with results of flight tests of the YP-80A airplane and wind-tunnel tests of a 1/3-scale model of the YP-80A.

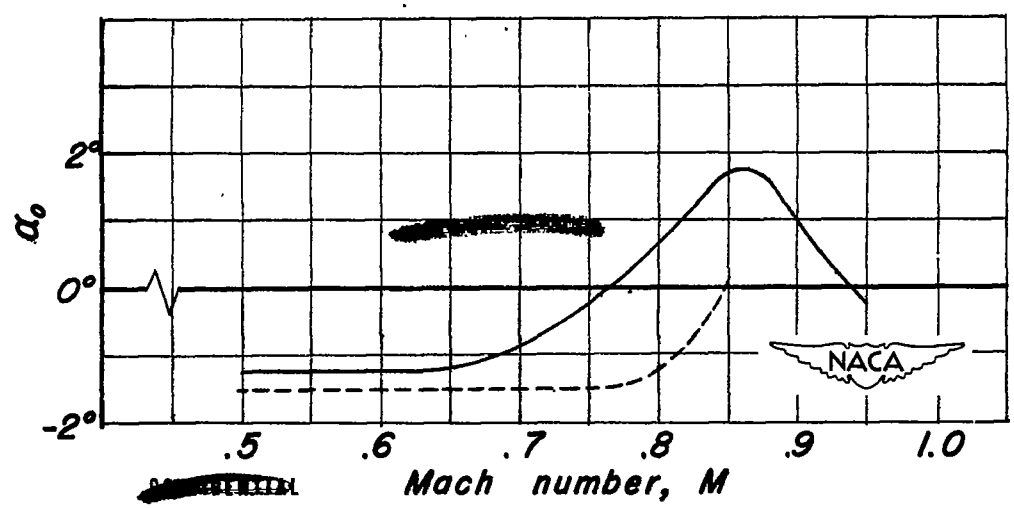

Figure 16.- Comparison of variation in angle of zero lift with Mach number for the 1/78-scale model of the YP-80A with results of wind-tunnel tests of a 1/3-scale model of the YP-80A airplane.

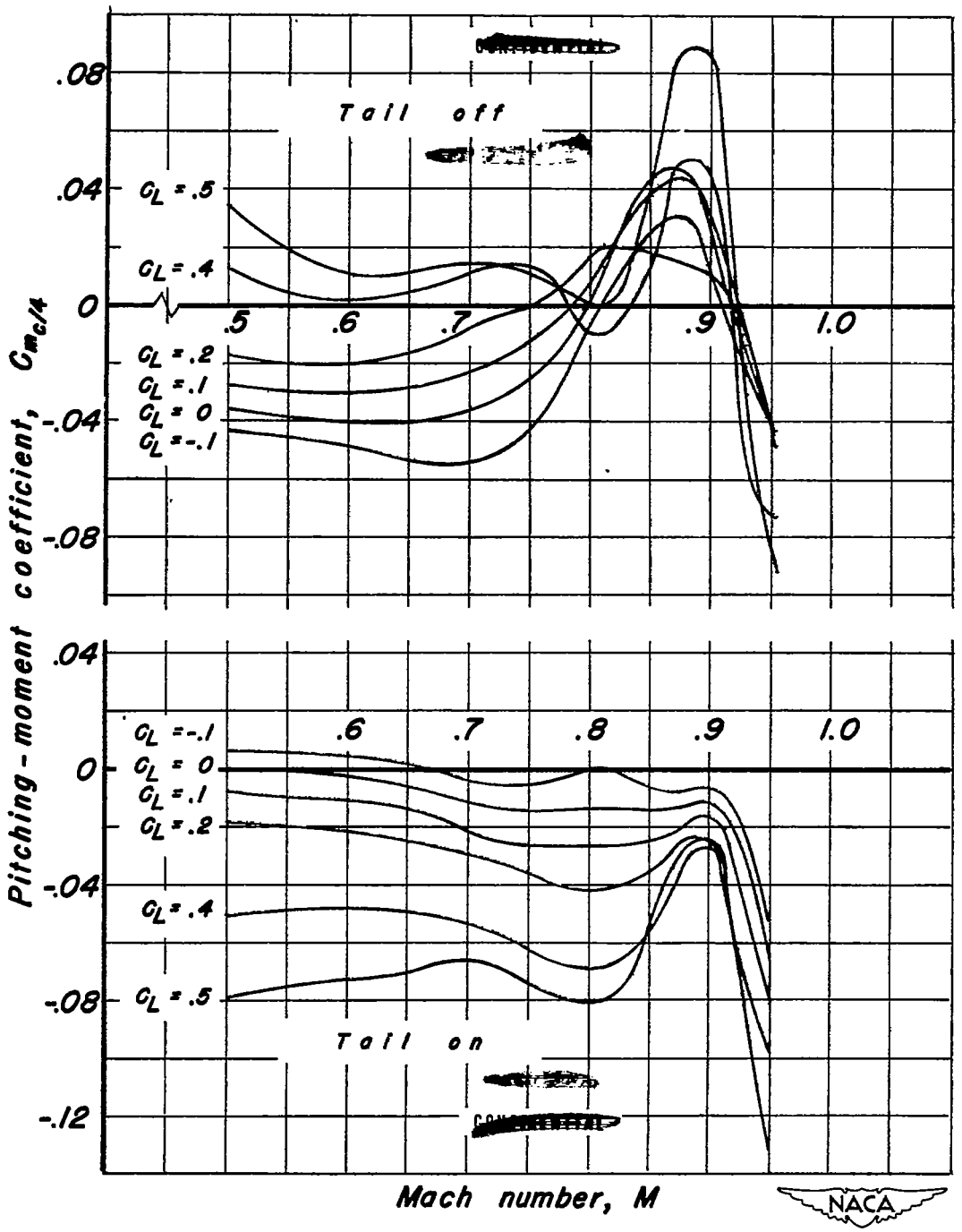

Figure 17.- Variation of pitching-moment coefficient with Mach number for the 1/78-scale model of the YP-80A airplane.

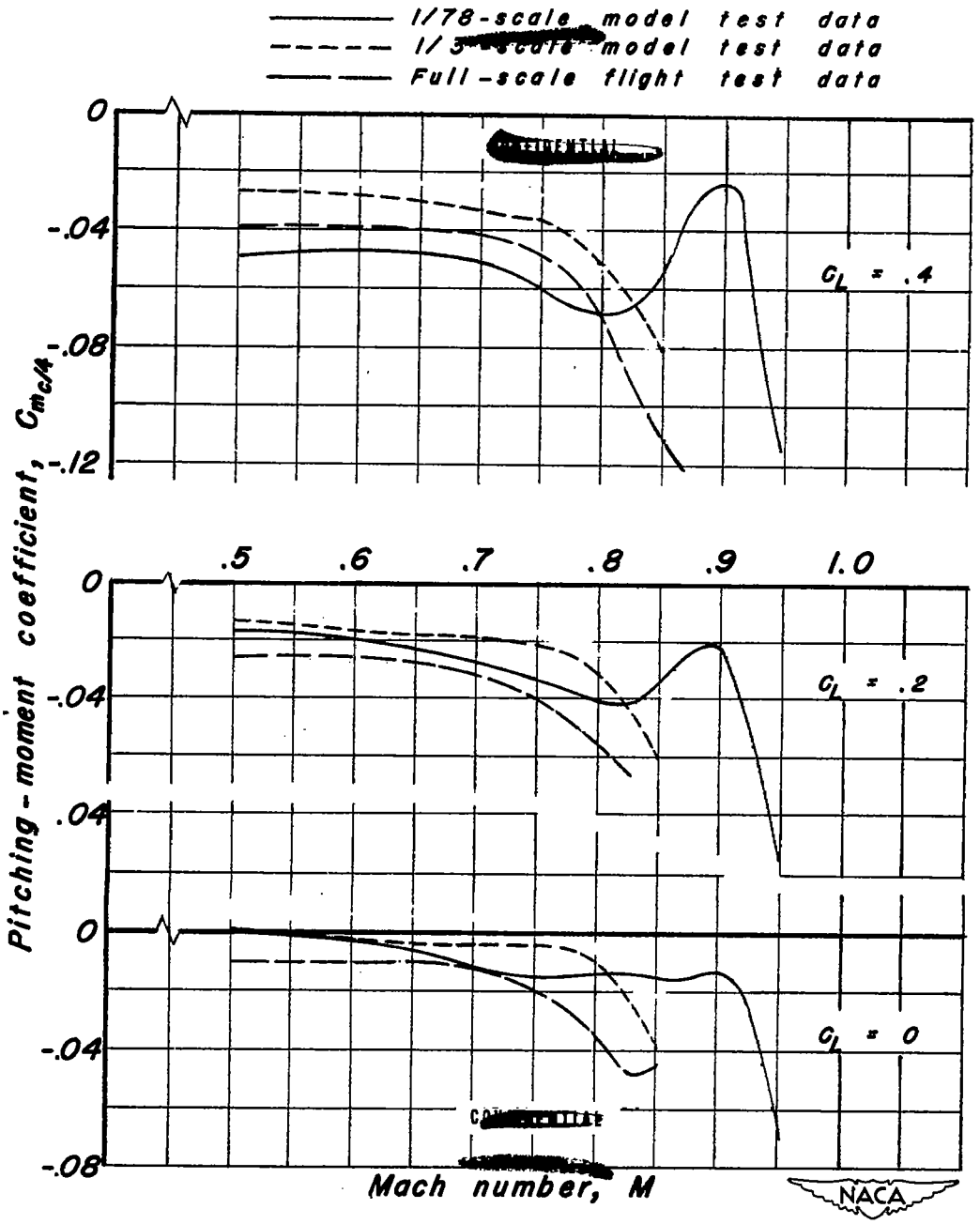

Figure 18.- Comparison of the variation in pitching-moment coefficient with Mach number for the 1/78-scale model of the YP-80A with results of flight tests of the YP-80A airplane and wind-tunnel tests of a 1/3-scale model of the YP-80A.

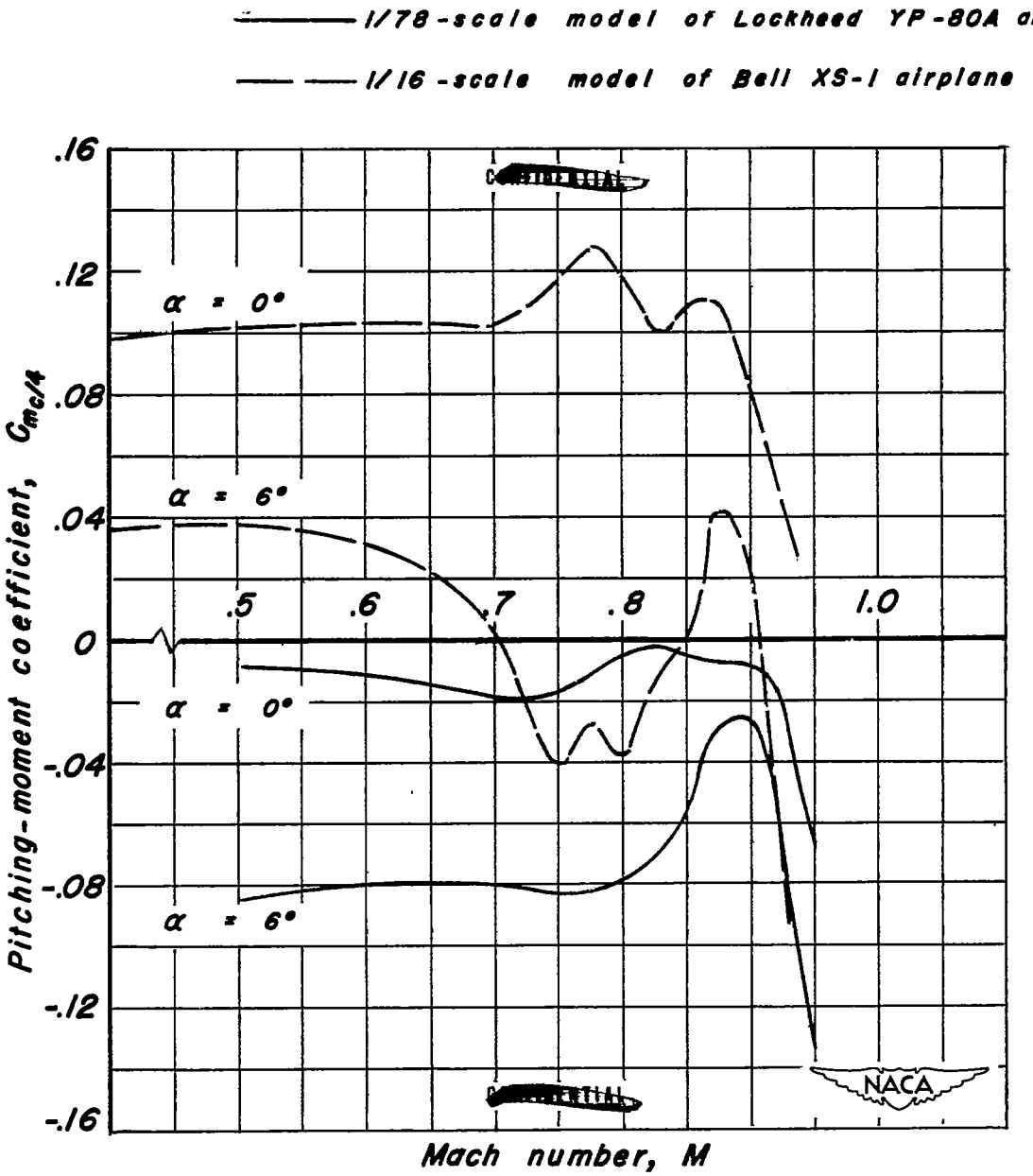

Figure 19.- Comparison of the variation of pitching-moment coefficient with Mach number for the 1/78-scale model of the Lockheed YP-80A airplane with that of the 1/16.-scale model of the Bell XS-1 airplane.

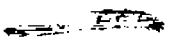

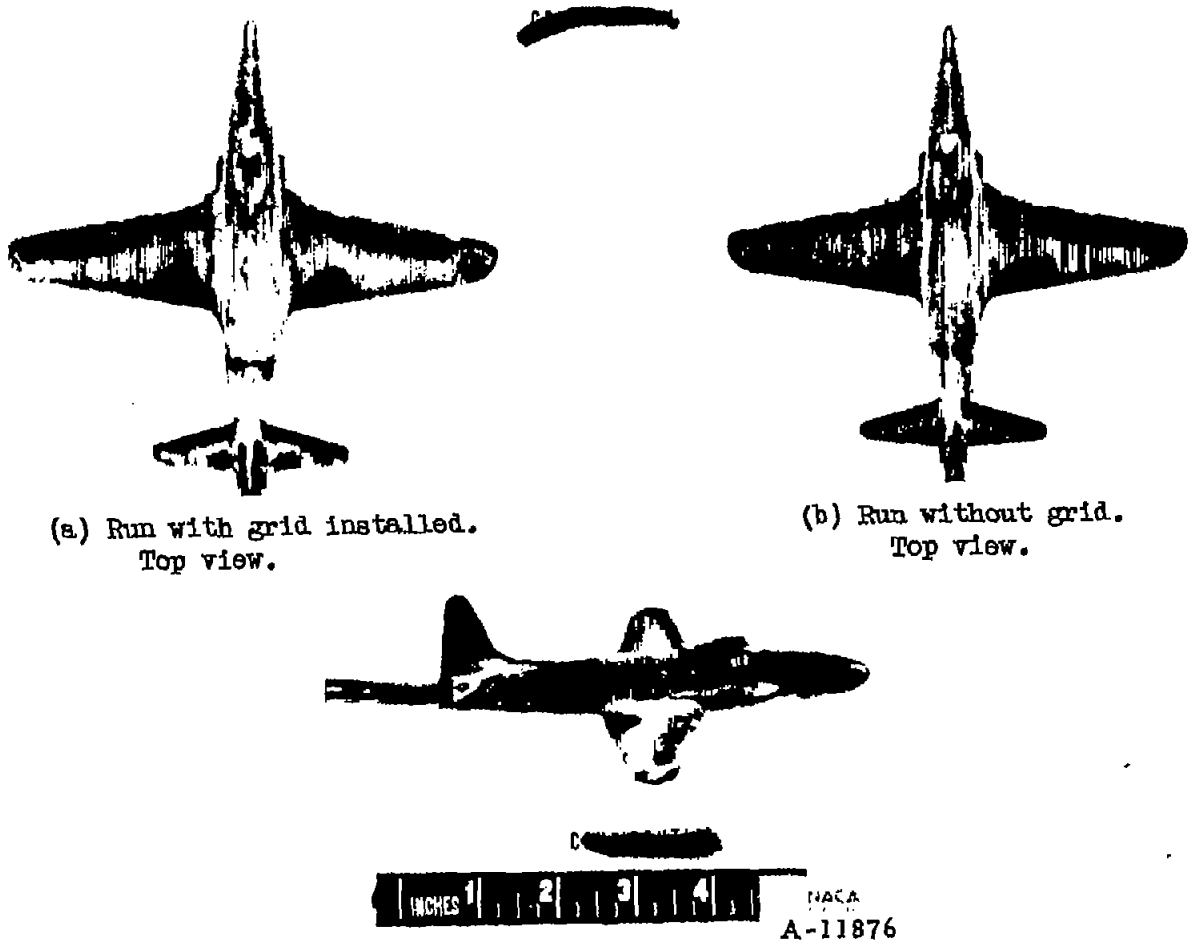

(a) Run with grid installed.
Top view.

(b) Run without grid.
Top view.

(c) Run with grid installed.
Side view.

Figure 20.– Flow pattern for the 1/78-scale model of the YP-80A airplane as indicated by the liquid-film method for measuring transition. Angle of attack, 4°; Mach number 0.6.

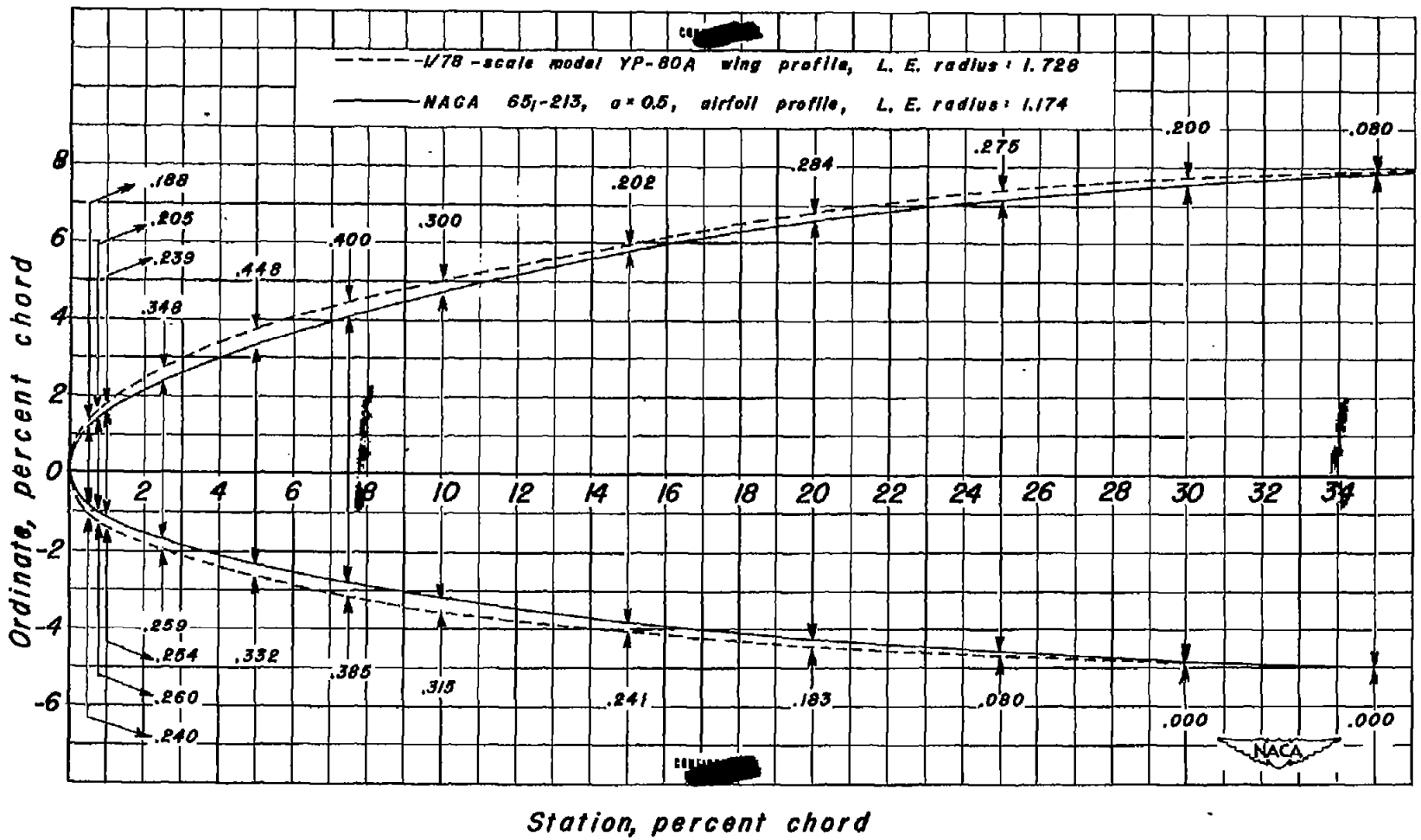

Figure 21.- Comparison of N.A.C.A. 65₁-213 profile with the wing section of the 1/78-scale model of the YP-80A airplane. (All stations, ordinates, and variations in percent chord.)

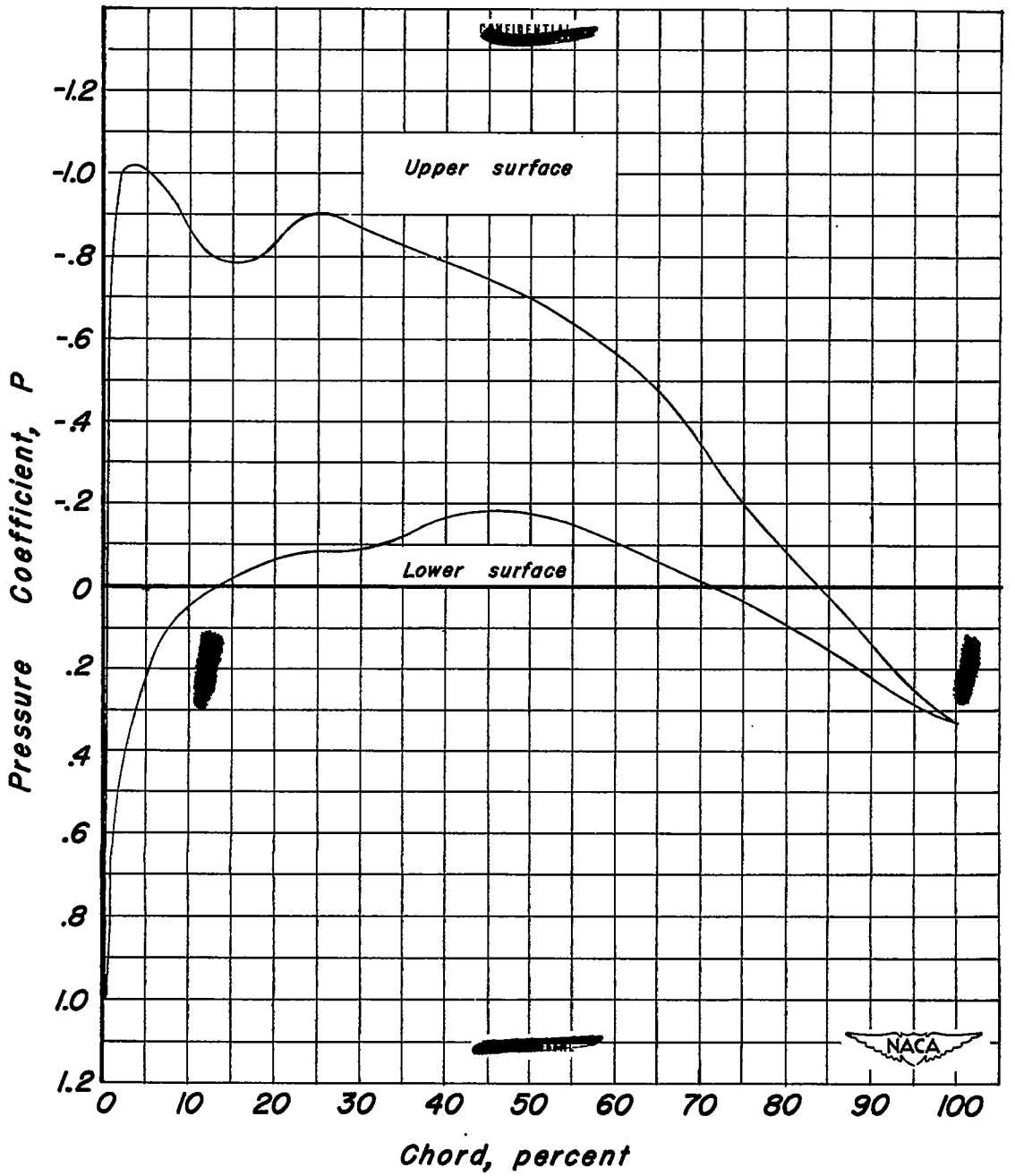

Figure 22.- Theoretical pressure distribution for the measured wing section of the 1/78-scale model of the YP-80A airplane. Angle of attack, 4°; Mach number, 0.6.

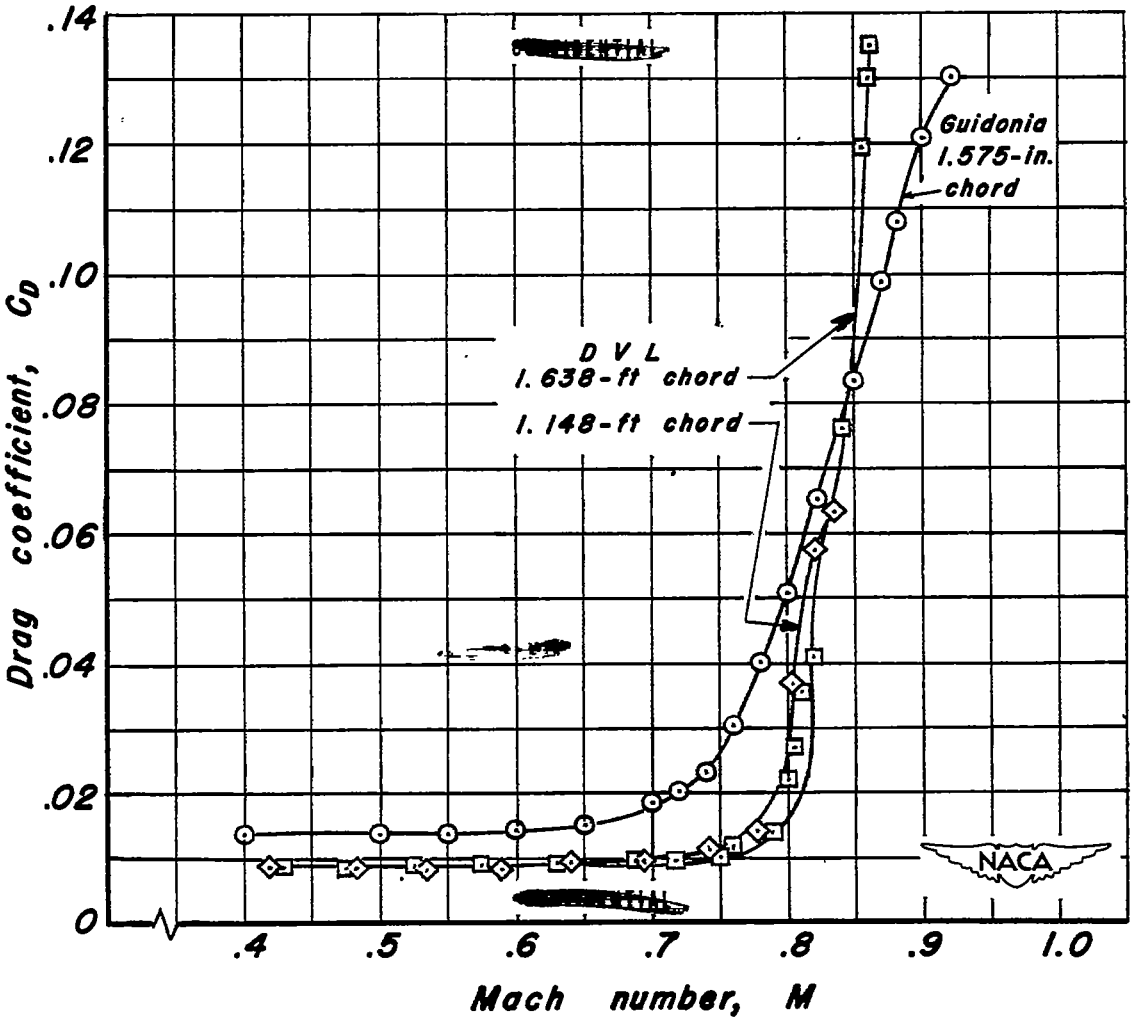

Figure 23.- Comparison of variation of drag coefficient with Mach number for an NACA 0015- 64 airfoil with results of tests made in the German DVL tunnel. $\alpha = 0°$

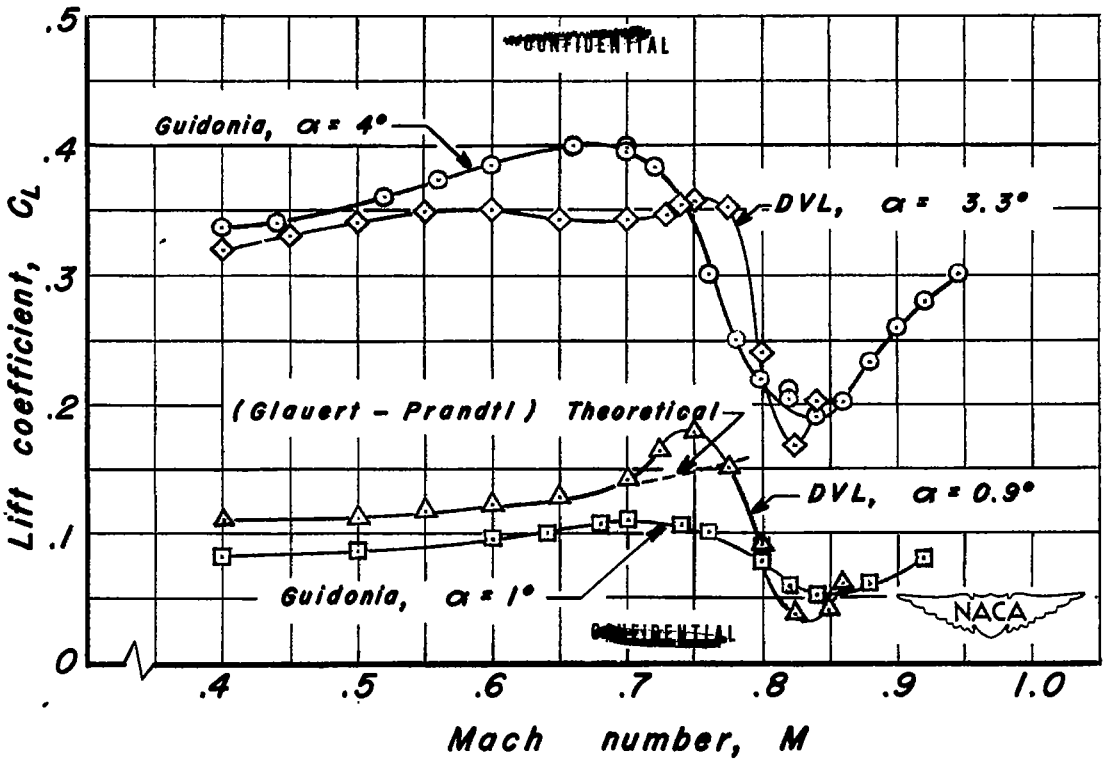

Figure 24.- Comparison of variation of lift coefficient with Mach number for an NACA 0015- 64 airfoil with results of tests made in the German DVL tunnel.

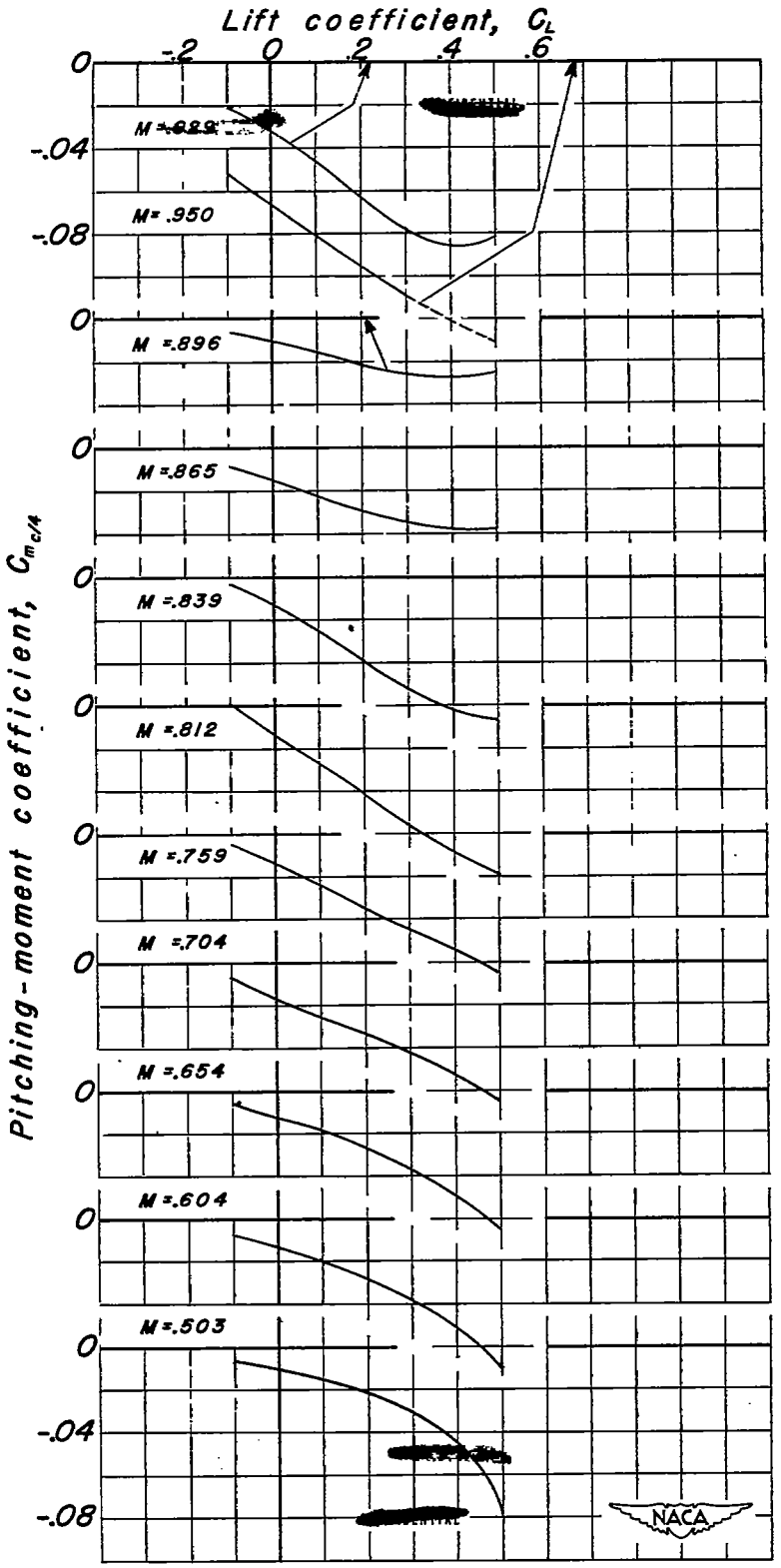

Figure 25.- Variation in pitching-moment coefficient with lift coefficient for the 1/78-scale model of the YP-80A airplane.

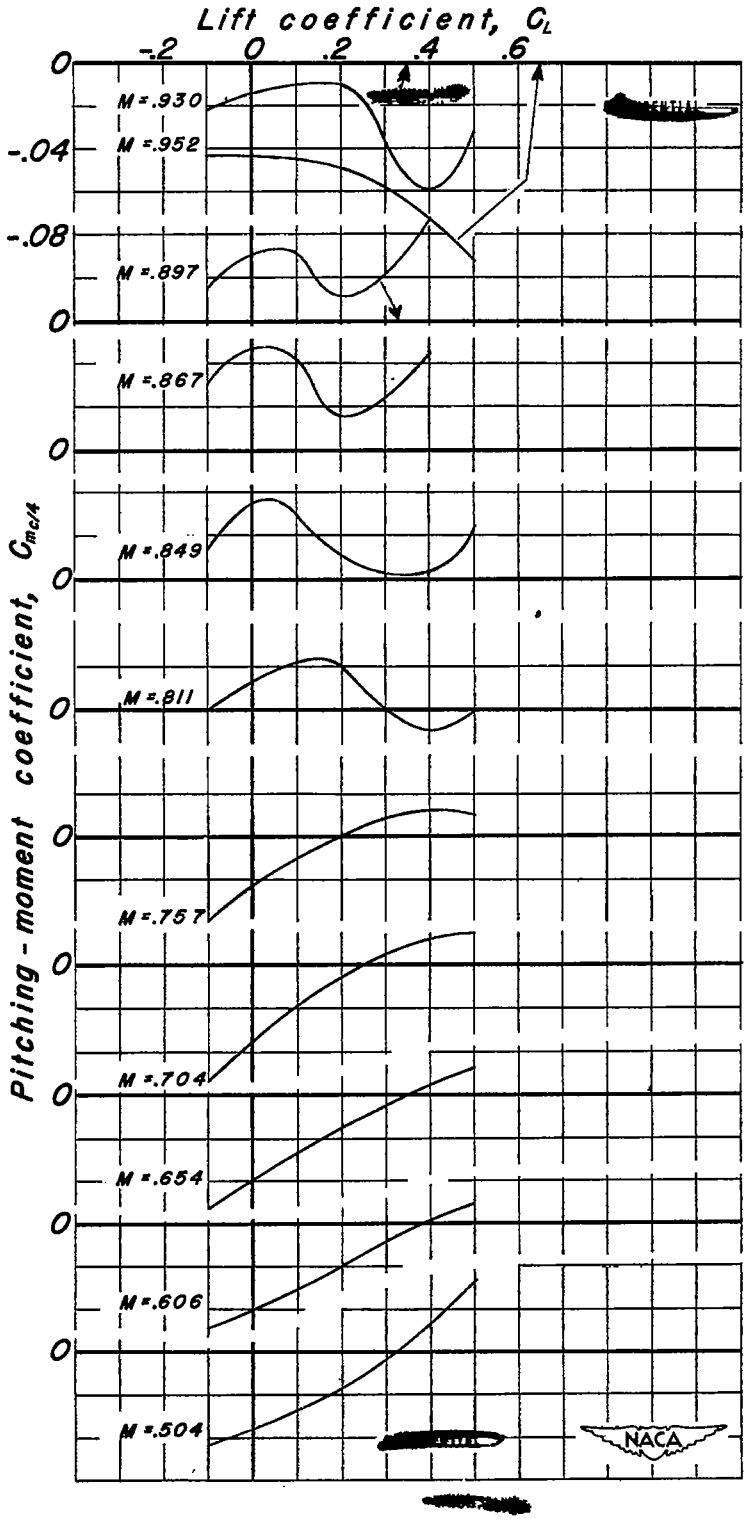

Figure 26.- Variation of pitching-moment coefficient with lift coefficient for the 1/78-scale model of the YP-80A airplane with tail off.

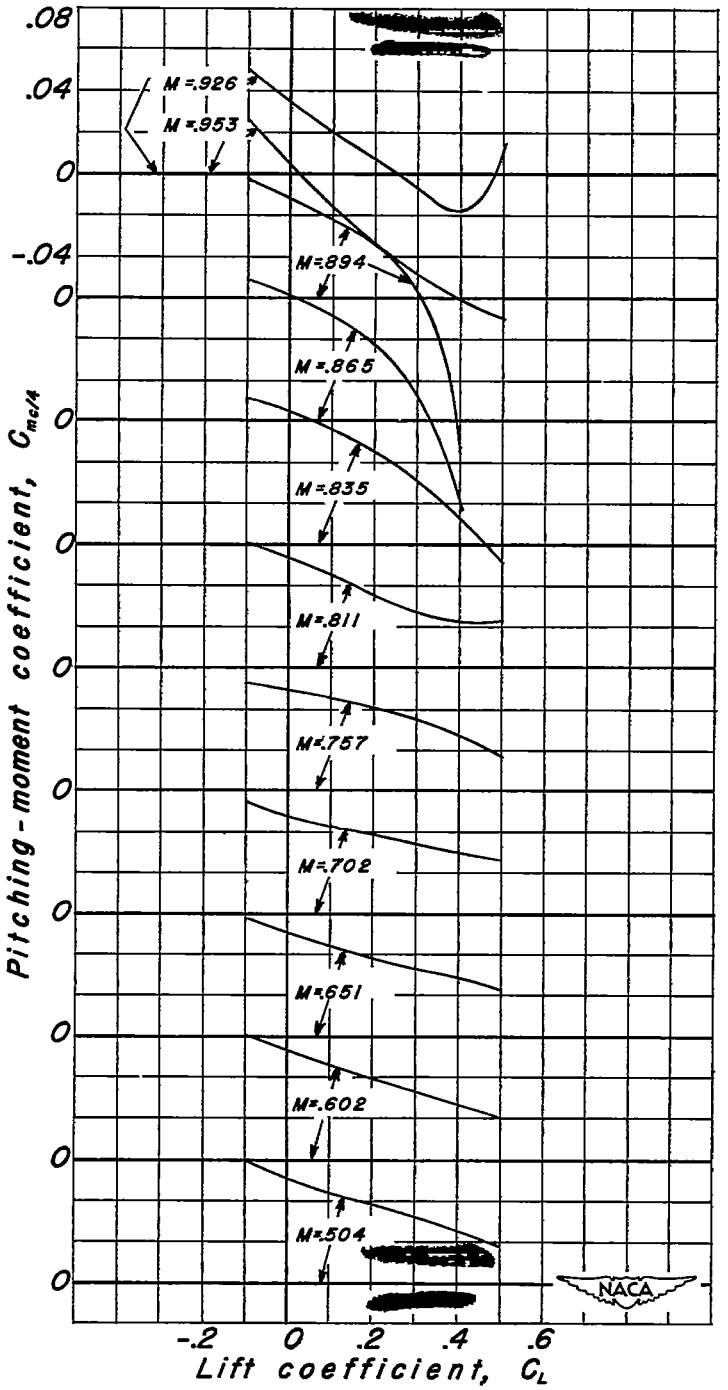

Figure 27.- Variation of pitching-moment coefficient with lift coefficient for the 1/78-scale model of the YP-80A airplane with 45° swept-back horizontal and vertical tail surfaces.

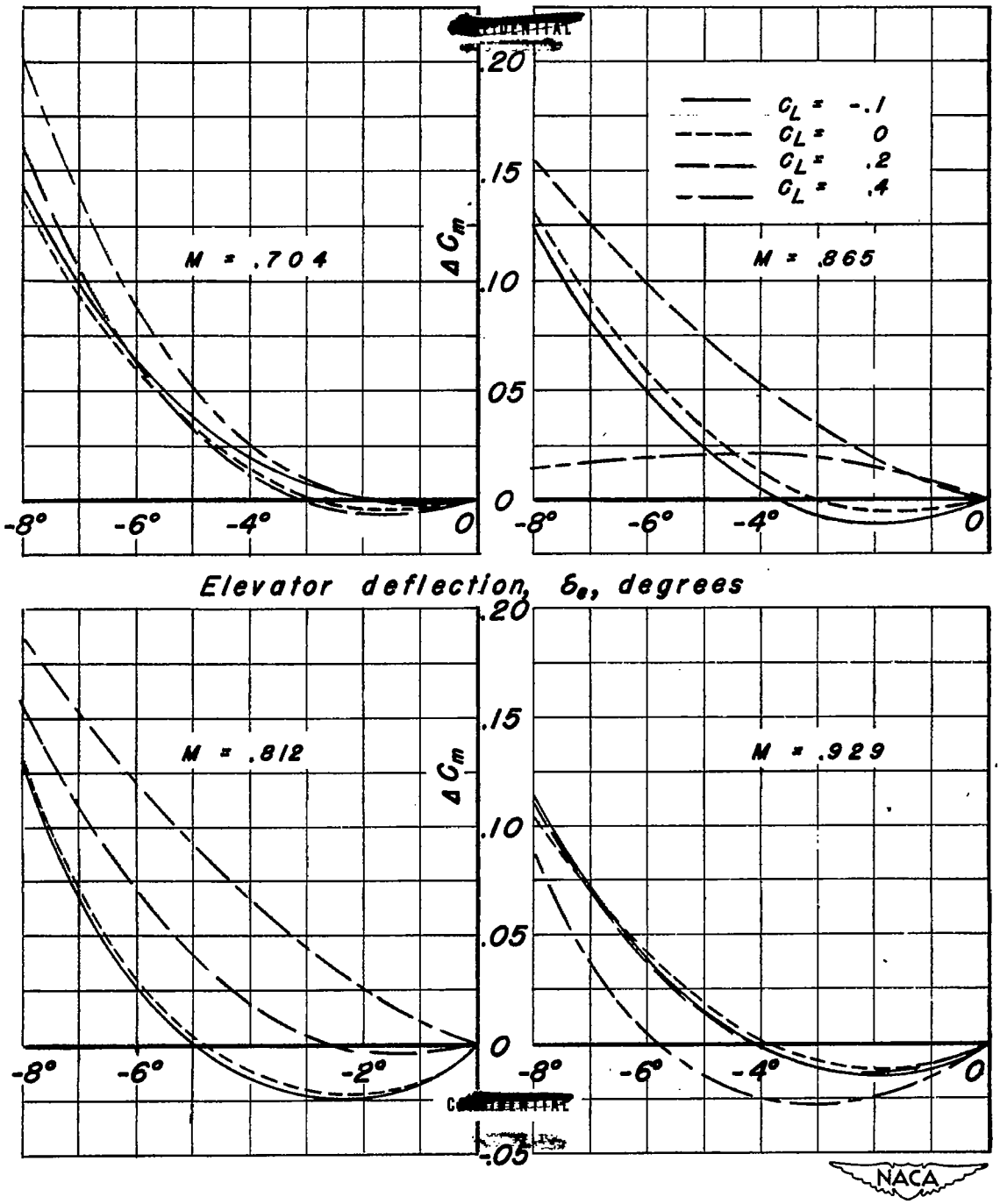

Figure 28.- Elevator effectiveness for the 1/78-scale model of the YP-80A airplane.